To the Graduate Council:

I am submitting herewith a thesis written by Weng Lock Kang entitled "A Microwave Plasma Closing Switch And Stealth Plasma Antenna." I have examined the final copy of this thesis for form and content and recommend that it be accepted in partial fulfillment of the requirements for the degree of Master of Science, with a major in Electrical Engineering.

Igor Alexeff
____
Igor Alexeff, Major Professor

We have read this thesis
and recommend its acceptance:

Marshall Pace
____

David Rosenberg
____

Accepted for the Council:

____
Associate Vice Chancellor and
Dean of The Graduate School

8

STATEMENT OF PERMISSION TO USE

In presenting this thesis in partial fulfillment of the requirements for a Master's degree at The University of Tennessee, Knoxville, I agree that the Library shall make it available to borrowers under the rules of the Library. Brief quotes from this thesis are allowable without special permission, provided that accurate acknowledgment of the source is made.

Permission for extensive quotation from or reproduction of this thesis may be granted by my major professor, or in his absence, by the Head of Interlibrary Services when, in the opinion of either, the proposed use of the material is for scholarly purposes. Any copy or use of the material in this thesis for financial gain shall not be allowed without my written permission.

Signature Weng Li Kang

Date 7/28/95

A MICROWAVE PLASMA CLOSING SWITCH AND STEALTH PLASMA ANTENNA

A Thesis
Presented for the
Master of Science
Degree
The University of Tennessee, Knoxville

Weng Lock Kang
August 1995

DEDICATION

In memory of my parents

I dedicate this thesis

to

my brothers and sisters

and

their families

ACKNOWLEDGMENTS

I wish to thank my advisor, Professor Igor Alexeff, for the help and support he has given me. I also wish to thank Professor Marshall Pace for his patience and advice, and Professor David Rosenberg for his encouragement.

There are a number of other people whose assistance should be acknowledged here. I would therefore like to thank Doctor Mark Rader for his invaluable suggestions on how to conduct a research, Doctor Mounir Laroussi and Doctor Paul Spence for their sharing of their knowledge in the field of plasma science.

Last but not least, I would like to thank Professor J. Reece Roth for the graduate courses he has taught me in the field of plasma science and engineering. His endless effort in organizing a weekly plasma seminar is greatly appreciated because the seminar has benefited me a lot.

ABSTRACT

We have successfully constructed a microwave plasma closing switch and a stealth plasma antenna using ordinary fluorescent tubes. For the microwave plasma closing switch, the basic idea is a coaxial plasma line structure the inner conductor of which is a fluorescent tube while the outer conductor is a metal pipe. Under normal conditions when the gas is not ionized, the system is just a waveguide beyond cutoff and microwave transmission is negligible. However, when the gas is ionized, the structure acts as an excellent coaxial line that transmits microwave. We have obtained a 63 dB relative amplitude for a 15 MHz signal and a 21 dB relative amplitude for a 900 MHz signal. By using a simple equivalent electrical circuit, we are able to predict the behavior of the coaxial line structure successfully. For the stealth antenna, the basic principle is based on the electromagnetic wave propagating in a plasma medium. If the incident wave frequency is greater than the plasma frequency, the wave will propagate through the tube. If the incident wave frequency is less than the plasma frequency, reflection will take place. However, when the gas is de-ionized, the radar cross section is negligible, rendering the antenna a stealth property. Our experimental work has successfully demonstrated the case.

TABLE OF CONTENTS

CHAPTER **PAGE**

LIST OF FIGURES

FIGURE **PAGE**

Chapter 1

INTRODUCTION

We have investigated, theoretically and experimentally, the feasibility of developing a microwave plasma closing switch and a stealth plasma antenna by using an ordinary fluorescent tube [1.1],[1.2] .

In chapters 2 to 5, we will describe our work on the microwave plasma closing switch. Chapters 6 to 8 will be devoted to the development of the stealth plasma antenna.

For the microwave plasma closing switch, we start with the basic idea in chapter 2. In chapter 3, we describe the experimental set-up and the procedures. Results from that experimental work will be presented in chapter 4. Finally, in chapter 5, we will attempt to find the theoretical and experimental fit.

For the stealth plasma antenna, the basic idea will be presented in chapter 6. While chapter 7 describes our experimental work, chapter 8 concludes our investigation by analyzing the experimental results.

A final chapter, chapter 9, concludes our overall findings. The short-comings of our investigation will be discussed and possible further study will be suggested.

It should also be mentioned here that unless otherwise specified, the equations and units used in this thesis are that of the SI systems.

Chapter 2

MICROWAVE PLASMA CLOSING SWITCH

a) Basic Idea

We are interested in the behavior of a plasma coaxial line in which the center conductor is a glass tube filled with a low pressure gas, and the outer conductor is a metal pipe.

Under the condition that the gas is not ionized, this structure corresponds to a cylindrical waveguide beyond cutoff and microwave transmission along the structure is negligible.

However, how will the structure behave when the gas in the cylindrical glass tube is ionized ? Will the glass tube behave as an excellent conductor, and the structures behave as a coaxial line that efficiently transmits microwave ?

During our studies, we found out that the answer is affirmative, and the structure can be used as a microwave plasma closing switch. We have found that an ordinary fluorescent lamp can be used as the central conductor.

b) Equivalent Electrical Circuit

Our plasma coaxial line structure can be represented in Figure 2.1. Note that the central conductor is an ordinary fluorescent tube with a radius a and the outer conductor is a metal pipe with a radius b. This coaxial line structure can be easily represented by an equivalent electrical circuit.

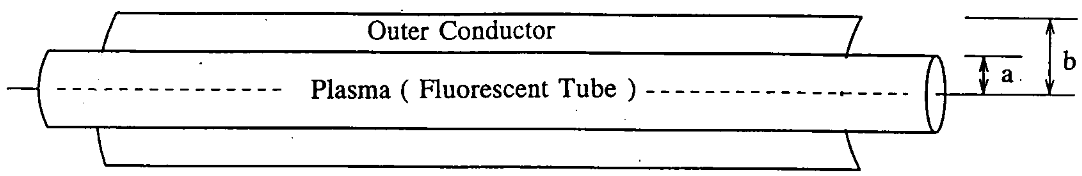

Figure 2.1 The Cylindrical Coaxial Plasma Line Structure.

The coaxial fluorescent tube and the outer conductor pipe behave like a parallel plate configuration and thus can be represented by a capacitance. The plasma itself is a lossy medium and can be represented by a series combination of resistors and inductors.

Thus, the plasma coaxial line structure can be viewed as a building block consisting of an infinite number of a simple equivalent circuit made up of resistor R, inductor L, and capacitor C as shown in Figure 2.2. Our task then is to analyze this equivalent circuit, particularly in the transmission ability of an incident signal through the structure.

c) Wave Equation

We now try to derive the wave equation for the equivalent electrical circuit by letting the voltages at points a, b, and c be $V(x-\Delta x)$, $V(x)$, and $V(x+\Delta x)$ respectively.

Thus, the voltage drop between points a and b can be expressed as

$$V(x-\Delta x)-V(x)=L\frac{di_1}{dx}+Ri_1 \tag{2.1}$$

The voltage drop between points c and b can be expressed as

$$V(x+\Delta x)-V(x)=L\frac{di_2}{dx}+Ri_2 \tag{2.2}$$

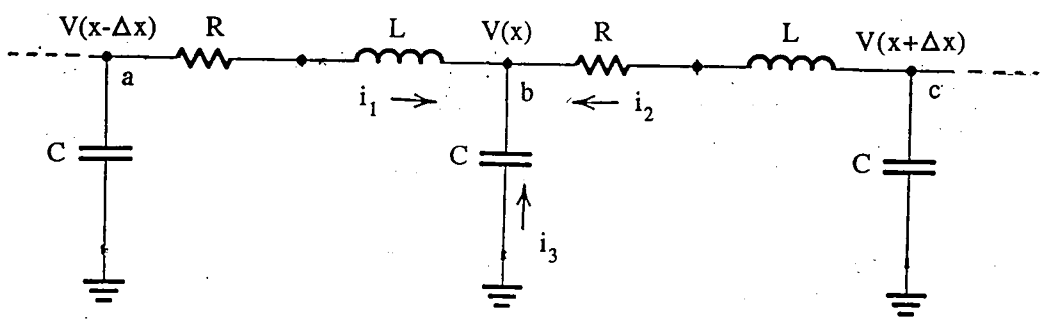

Figure 2.2 The Equivalent Electrical Circuit for the Coaxial Plasma Line Structure.

whereas the voltage drop due to capacitor C is

$$-C\frac{dV(x)}{dt} = i_3 \tag{2.3}$$

We now assume that the voltage and current have the following forms of solution

$$V = V_0 e^{i(kx-\omega t)} \tag{2.4}$$

$$i = i_o e^{i(kx-\omega t)} \tag{2.5}$$

where k is the wave number and ω the incident radiant frequency. By substituting equations (2.4) and (2.5) into equations (2.1), (2.2), and (2.3), we get

$$V(x-\Delta x) - V(x) = (-i\omega L + R)i_1 \tag{2.6}$$

$$V(x+\Delta x) - V(x) = (-i\omega L + R)i_2 \tag{2.7}$$

$$i\omega C V(x) = i_3 \tag{2.8}$$

These currents can be added according to Kirchoff current law

$$i_1 + i_2 + i_3 = 0 \tag{2.9}$$

or

$$\frac{V(x-\Delta x) - 2V(x) + V(x+\Delta x)}{(-i\omega L + R)} + i\omega C V(x) = 0 \tag{2.10}$$

Next, we assume that the capacitance C, inductance L, and resistance R can be expressed in terms of Δx as

$$L = L_0 \Delta x, \quad C = C_0 \Delta x, \text{ and } \quad R = R_0 \Delta x \tag{2.11}$$

Thus, equation (2.10) becomes

$$\frac{V(x-\Delta x) - 2V(x) + V(x+\Delta x)}{C_0(-i\omega L_0 + R_0)(\Delta x)^2} + i\omega V(x) = 0 \tag{2.12}$$

In the limit of $\Delta x \to 0$, equation (2.12) becomes a differential equation as

$$\frac{\partial^2 V(x)}{\partial x^2} + (i\omega C_0 R_0 + \omega^2 C_0 L_0) V(x) = 0 \tag{2.13}$$

Actually, if we go back to equation (2.4), and differentiate the equation twice with respect to x, we get

$$\frac{\partial^2 V(x)}{\partial x^2} + k^2 V(x) = 0 \tag{2.14}$$

Equation (2.14) is the familiar wave equation.

By comparing equations (2.13) and (2.14), we get the complex wave number k

$$\begin{aligned} k^2 &= \omega^2 L_0 C_0 + i\omega C_0 R_0 \\ &= L_0 C_0 \omega^2 (1 + \frac{iR_o}{\omega L_0}) \end{aligned} \tag{2.15}$$

Thus,

$$k = \omega\sqrt{L_0 C_0}\sqrt{1+\frac{iR_0}{\omega L_0}}$$
$$\approx \omega\sqrt{L_0 C_0} + \frac{iR_0}{2\sqrt{L_0/C_0}} \quad \text{if} \quad \frac{R_0}{\omega C_0} \leq 1$$
$$= k_R + ik_I \tag{2.16}$$

where

$$k_R = \omega\sqrt{L_0 C_0} \tag{2.17}$$
$$k_I = \frac{R_0}{2\sqrt{L_0/C_0}} \tag{2.18}$$

We will later show that k_R is the sinusoidal portion whereas k_I is the damping portion of the voltage and current solutions.

The capacitance per unit length C_0, the inductance per unit length L_0, and the resistance per unit length R_0 will be determined next.

d) Determination of C_0

To determine C_0, let us consider an electric field $\vec{E}$ produced by an infinite uniform line charge density q_l as shown in Figure 2.3. Assuming q_l is parallel to the z axis, we have azimuthal symmetry and z independence, so that $\vec{E}$ is independent of ϕ and z. Thus $\vec{E}$ has only a radial component and can be expressed as [2.1]

$$\vec{E} = \frac{q_l}{2\pi\varepsilon_0\rho}\hat{\rho} \tag{2.19}$$

The corresponding potential V can be expressed as

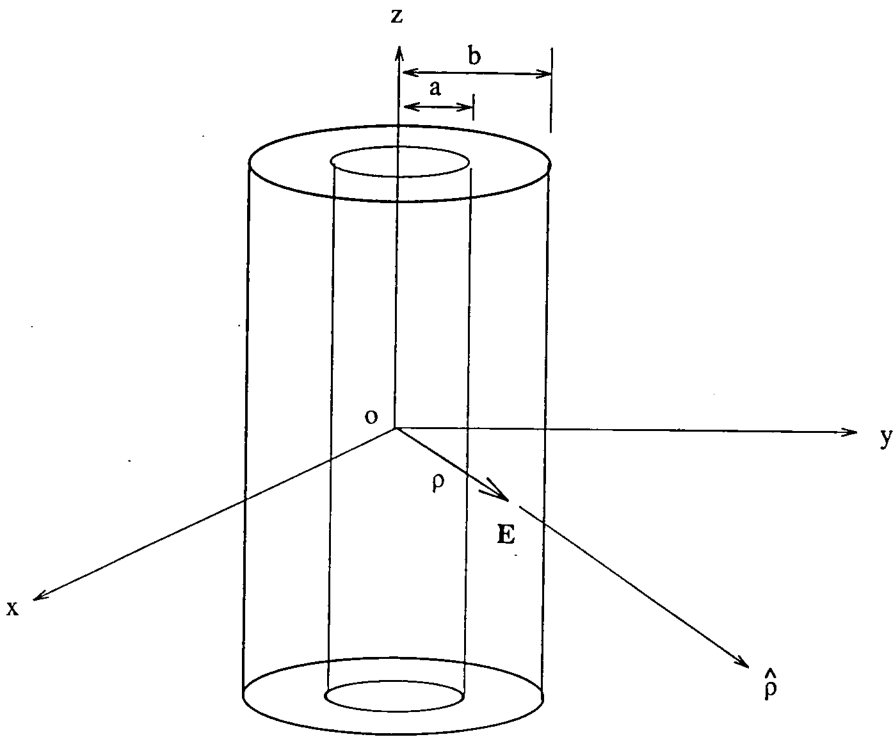

Figure 2.3 Finding C_o Between Two Coaxial Cylinders.

$$V = \frac{q_l}{2\pi\varepsilon_o} \ln(b/a) \tag{2.20}$$

Since q = C_oV, we finally get

$$C_0 = \frac{2\pi\varepsilon_0}{\ln(b/a)} \tag{2.21}$$

e) Determination of L_o

To determine L_o , let us consider a current i passing through a conducting cylindrical rod, as shown in Figure 2.4. The magnetic field $\vec{B}$ produced by such a current can be expressed as [2.2]

$$\vec{B} = \frac{\mu_o i}{2\pi\rho}\hat{\phi} \tag{2.22}$$

Now, Stokes' theorem [2.3] states that

$$\iint_s (\nabla \times \vec{E}) \bullet d\vec{s} = \oint_c \vec{E} \bullet d\vec{l} \tag{2.23}$$

where s is an open surface bounded by the closed path of c.

By applying Maxwell's equation, the left-hand-side of equation (2.23) becomes

$$\iint_s (\nabla \times \vec{E}) \bullet d\vec{s} = \iint_s (-\frac{\partial \vec{B}}{\partial t}) \bullet d\vec{s} \tag{2.24}$$

whereas the right-hand-side of equation (2.20) is just

$$\oint_c \vec{E} \bullet d\vec{l} = -V \tag{2.25}$$

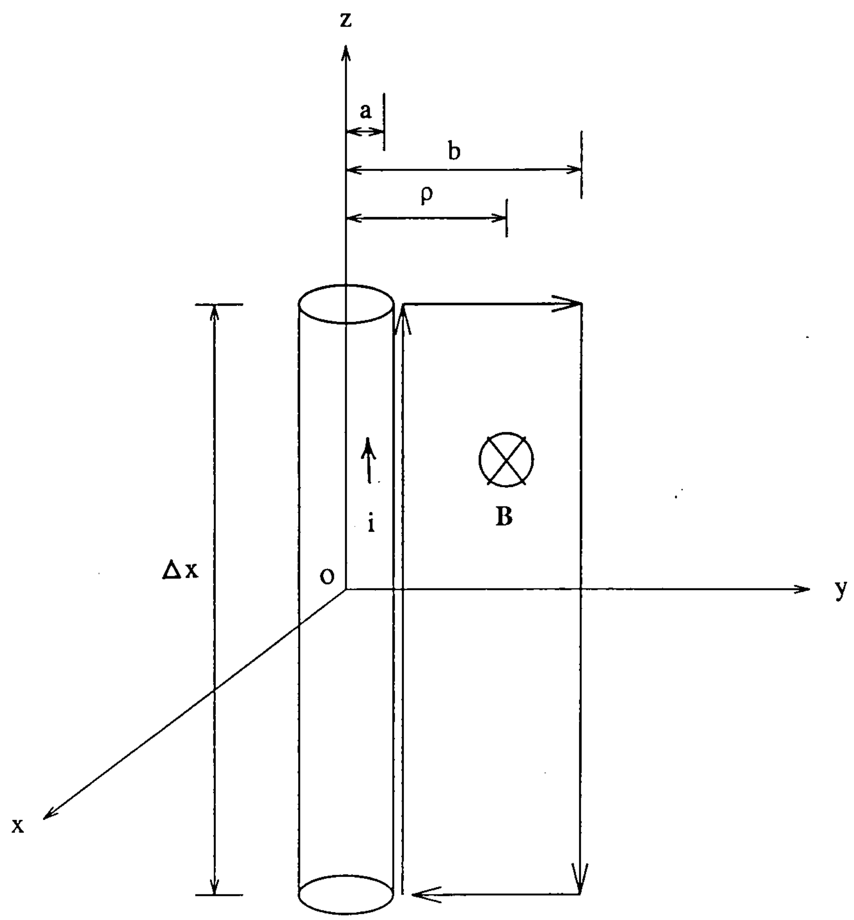

Figure 2.4 Finding L_o on a Conducting Cylindrical Rod.

Thus, equation (2.23) can be expressed a

$$\iint_s (-\frac{\partial \vec{B}}{\partial t}) \bullet d\vec{s} = V = L\frac{\partial i}{\partial t} \tag{2.26}$$

or

$$\frac{\mu_0}{2\pi}\frac{\partial i}{\partial t}\int_a^b \frac{d\rho}{\rho} = L_0 \frac{\partial i}{dt} \tag{2.27}$$

or

$$L_o = \frac{\mu_o}{2\pi}\ln(\frac{b}{a}) \tag{2.28}$$

f) Determination of R_o

To determine R_o , let us consider a column of plasma maintained by a dc potential difference of V as shown in Figure 2.5.

The current density j can be expressed as [2.4]

$$j = \frac{i}{A} = zen_e v \tag{2.29}$$

where i is the current, A the area, z the atomic number, n_e the electron density, and v the average electron velocity.

The average velocity v is given by

$$v = \frac{zeEt_c}{2m} \tag{2.30}$$

where m is the mass of an electron, and t_c the collision time. For an industrial plasma device such as a fluorescent tube, this collision frequency is that due to the electron-neutral collision . The equation for t_c is [2.5]

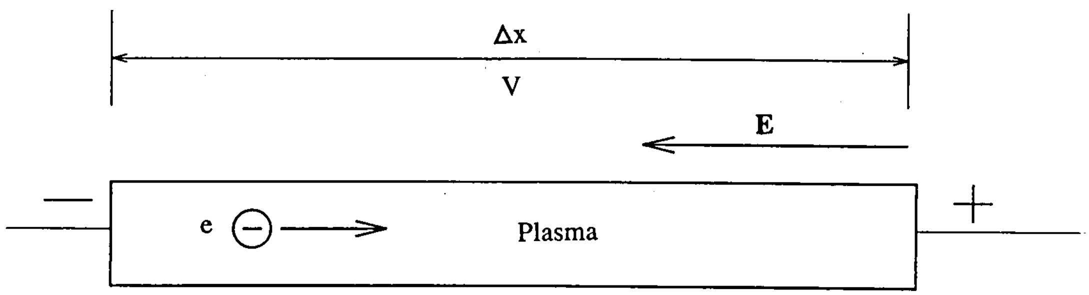

Figure 2.5 Finding R_o in a Column of Plasma.

$$t_c = \frac{l_f}{v_t} \qquad (2.31)$$

where l_f is the mean free path and v_t the thermal velocity. The equations for l_f [2.6] and v_t [2.7] are

$$l_f = \frac{1}{n_g \sigma} \qquad (2.32)$$

and

$$v_t = \sqrt{\frac{kT_e}{m}} \qquad (2.33)$$

where n_g is the density of the neutral gas, σ the collision cross section, k the Boltzmann's constant, and T_e the electron temperature.

If we substitute equations (2.31),(2.32), and (2.33) into equation (2.30), we get

$$v = \frac{zeE}{2mn_g\sigma\sqrt{kT_e/m}} \qquad (2.34)$$

We now substitute equation (2.34) into equation (2.29) to get

$$i = \frac{z^2e^2n_eAE}{2mn_g\sigma\sqrt{\frac{kT_e}{m}}} \qquad (2.35)$$

But $$R_0 = \frac{V}{i\Delta x} = \frac{E}{i} \qquad (2.36)$$

Thus, from equations (2.35) and (2.36) , we finally get

$$R_0 = \frac{2mn_g\sigma\sqrt{kT_e/m}}{z^2e^2n_eA} \tag{2.37}$$

g) Expression for V

From the previous sections, we have

$$V = V_0 e^{i(kx-\omega t)} \tag{2.4}$$

and
$$k = \omega\sqrt{L_0C_0} + \frac{iR_0}{2\sqrt{L_0/C_0}} \tag{2.16}$$

By substituting equation (2.16) into (2.4), we have

$$V = V_0 e^{i(\omega\sqrt{L_0C_0}x-\omega t)} e^{-\frac{R_0x}{2\sqrt{L_0/C_0}}} \tag{2.38}$$

In a steady state, the solution for V becomes

$$V = V_0 e^{-\frac{R_0x}{2\sqrt{L_0/C_0}}} \tag{2.39}$$

This suggests that the amplitude of the incident wave is damped. An alternative expression for equation (2.39) is

$$V = V_0 e^{-\frac{aL_t i_{av}}{2\sqrt{L_0/C_0}\,i}} \tag{2.40}$$

where L_t is the length of the tube, i_{av} the reference average current through the tube, a the voltage drop per unit length of the tube. Note that i_{av}/i has the unit of 1/ampere where i_{av} carries no unit.

Chapter 3

EXPERIMENTAL SET-UP FOR THE CLOSING SWITCH

a) Experimental Set-up

The experimental set-up of the coaxial plasma line structure is shown in Figure 3.1. whereas the photo version of it is shown in Figure 3.2.

The equipment used include the following:

1. Power Supply: A Lambda Electronics Corp.'s Regulator power supply, model 50, with dc voltage output of 0-500 volts, and dc current output of 0-500 mA.

2. Spectrum Analyzer

a.) a Tektronix 1L10 spectrum analyzer plug in unit connected to a Tektronix 546 oscilloscope (operating range is 2-36MHz) for analyzing signal below 30 MHz.

b) a Tektronix type 491 spectrum analyzer (operating range is 10MHz-4 GHz) for analyzing signal above 30 MHz.

3. R.F... Signal Generator:

a) a General Radio Company's bridge oscillator, type 1330A (operating range is 5kHz - 50MHz) for transmitting signal below 50MHz.

b). a General Radio Company's unit oscillator , type 1208C (operating range is 65-500MHz) for transmitting signal below 500MHz.

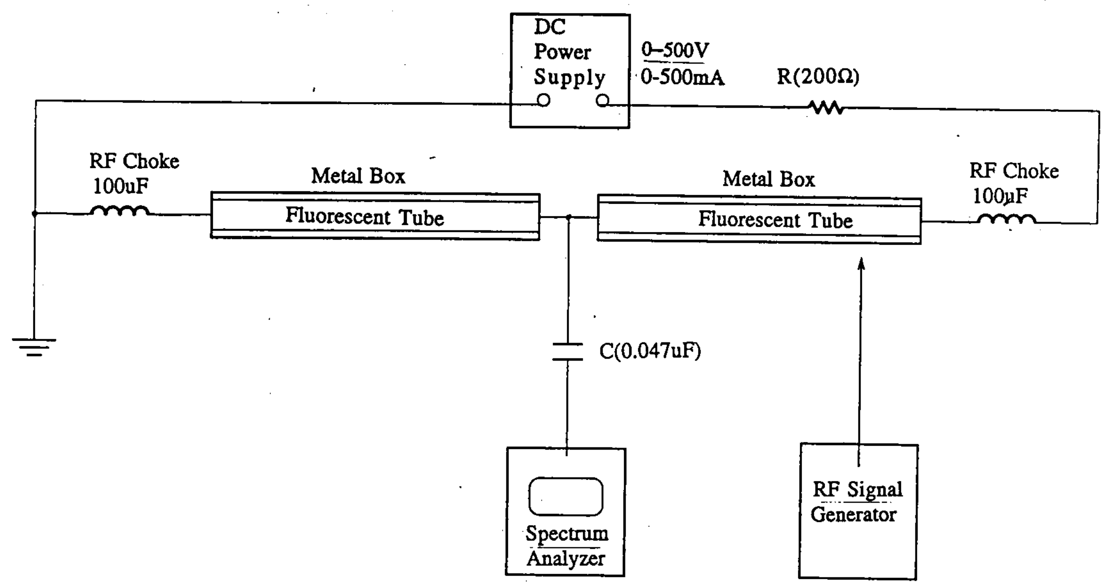

Figure 3.1 Schematic of the Coaxial Plasma Line Structure.

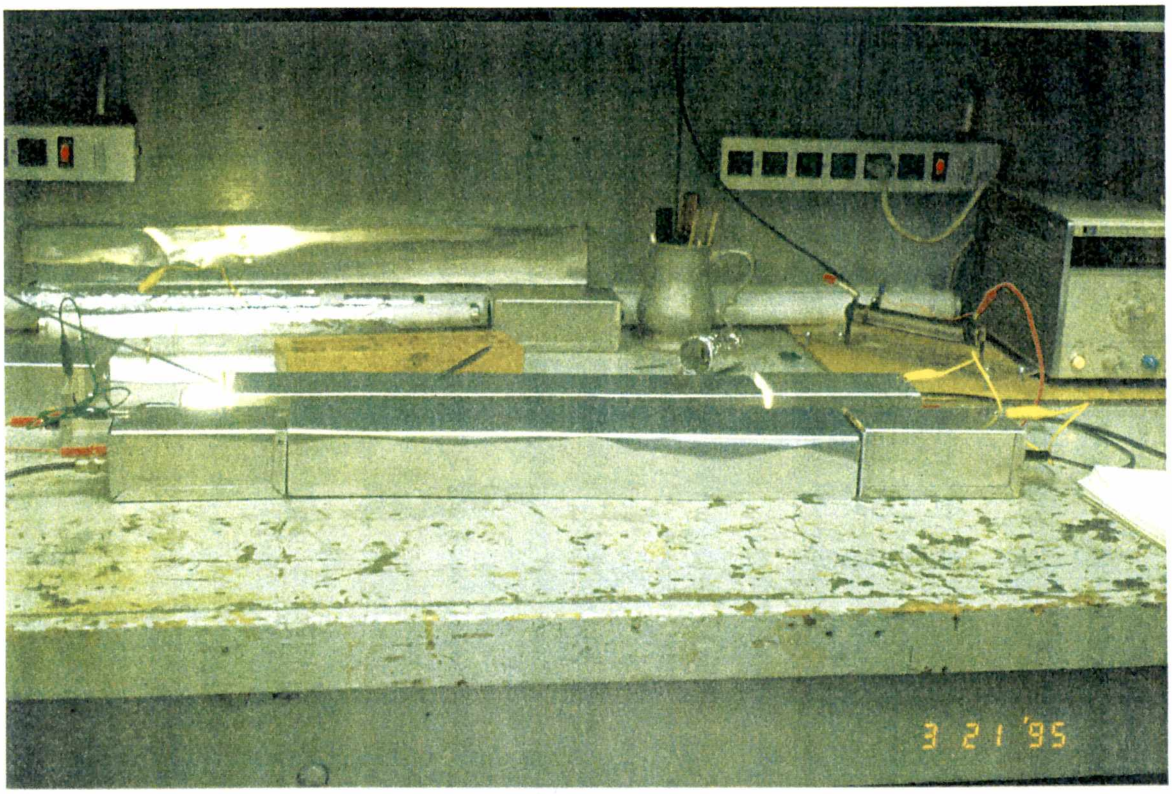

Figure 3.2 Photo of the Experimental Set-up.

c. a General Radio Company's unit oscillator, type 1209C (operating range is 250-960MHz) for transmitting signal above 500 MHz.

4. Fluorescent Tubes:

a). two 48"/40W, 1.5" diameter cool white tubes

b). two 24"/20W, 1.5" diameter cool white tubes

5. Other circuit elements such as resistance, rf chokes, and capacitors are specified in Figure 3.1.

b). V-I Characteristics Measurements

V-I characteristics measurements can be easily done by measuring the current through the tube and the voltage between the two ends of a tube.

c) Relative Amplitude Measurements

The relative amplitude measurement is what interested us. A relative amplitude of a signal is defined here as the amplitude difference between a signal when the gas is ionized compared to that when the gas is de-ionized. By measuring the relative amplitude, one would therefore know how well a signal is being transmitted through the coaxial plasma line structure.

The relative amplitude of a signal is measured through the following procedure [3.1] :

1. Center the IF CENTER FREQ. control. Switch out any IF Attenuation. Tune the signal without plasma on with the lowest amplitude of the screen.

2. Adjust the GAIN control so the low amplitude signal establishes a reference amplitude.

3. Now tune the signal with the plasma on to the center of the display. Add IF ATTENUATION until the signal amplitude decreases to the same reference amplitude established in step 2.

4. Add the total attenuation that was switched on. This is the relative amplitude difference, in dB, between the two compared signals.

Chapter 4

RESULTS AND ANALYSIS

a) V-I Characteristic Curve

The V-I characteristic curve of the 48"/40W tube is shown in Figure 4.1 whereas that of the 24"/20W tube is shown in Figure 4.2. They are plotted by the semilogy [4.1] function in MATLAB [4.2] .

Since the semilog plot reveals a linear relation between the voltage and current, the relationship of I and V can be expressed as

$$I = I_0 e^{-\alpha V} \tag{4.1}$$

For the 48" tube, α is estimated to be $6.07x10^{-2}$/volt and $4.11x10^{-2}$/volt for the lower and upper curve respectively. The temperatures are $1.9x10^5$ ^{0}k and $2.82x10^5$ ^{0}k respectively.

For the 24" tube, α is estimated to be $9.45x10^{-2}$/volt and temperature to be $1.23x10^5$ ^{0}k.

b) Relative Amplitude vs Current Curves

The relative amplitude vs current curves for the 48"/40W tube are shown in Figure 4.3 and Figure 4.4. Figure 4.3 represents the tube that is not covered by an outer conductor while Figure 4.4 represents that of a tube covered

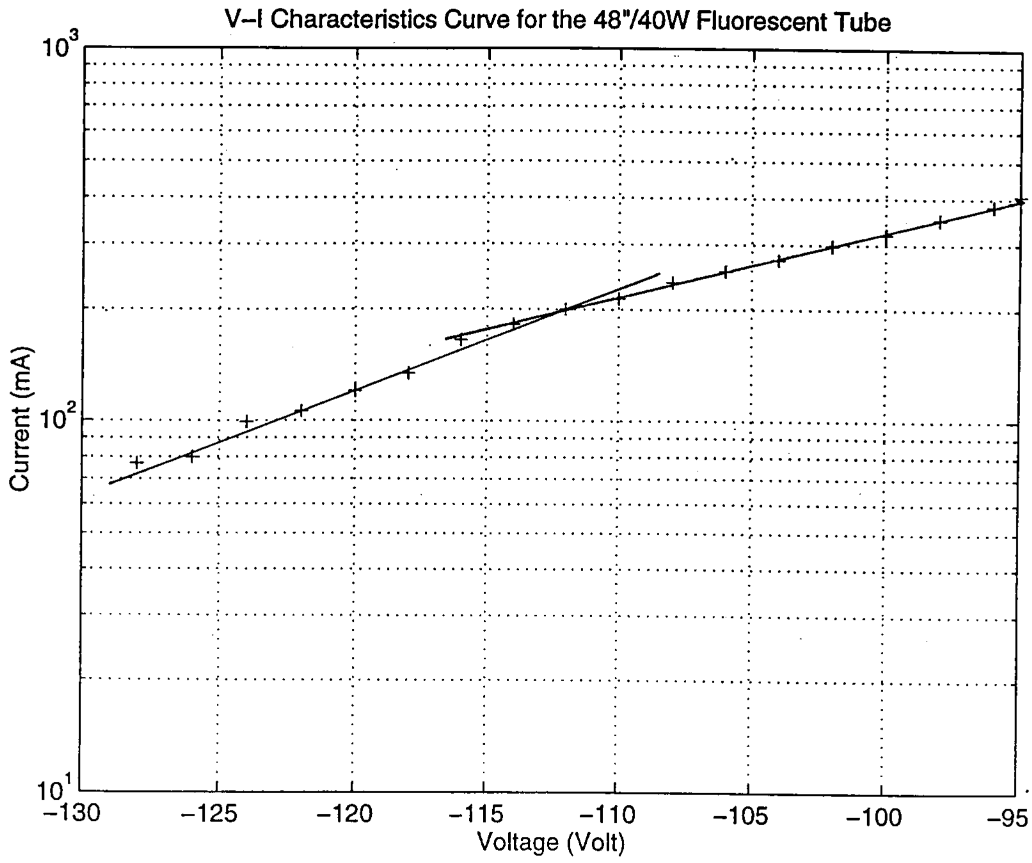

Figure 4.1 V-I Characteristic Curve for the 48"/40W Fluorescent Tube.

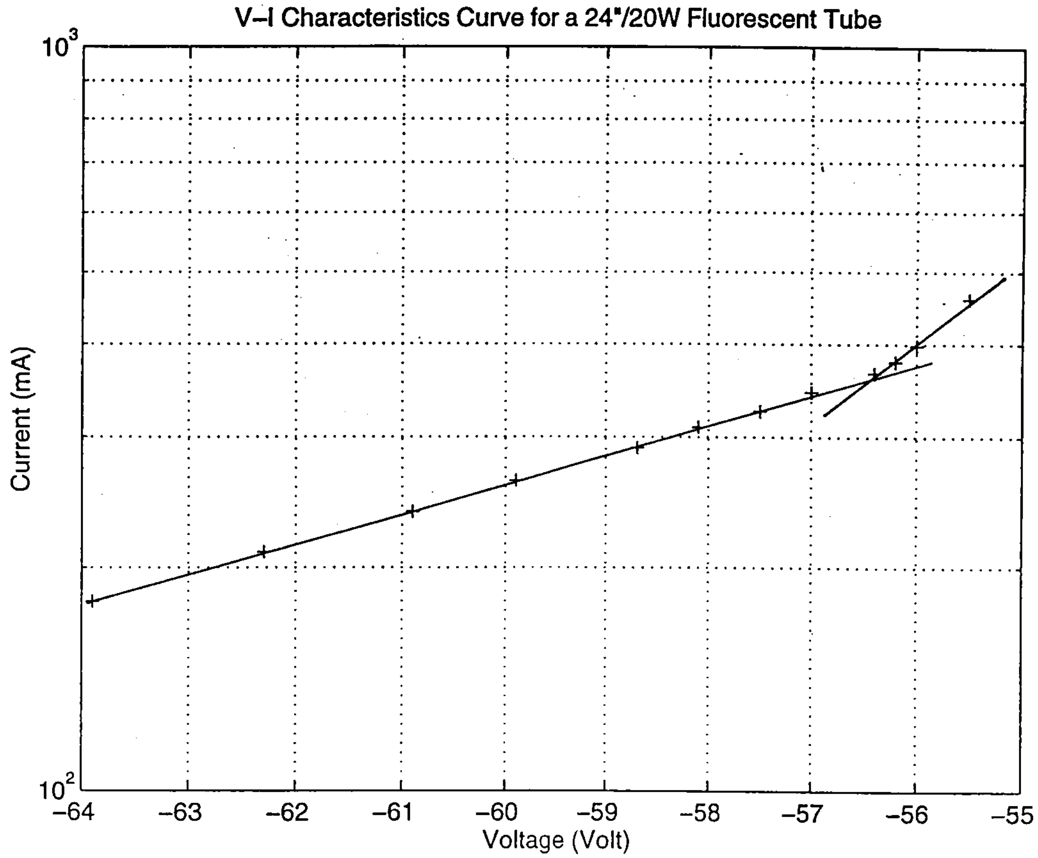

Figure 4.2 The V-I Characteristic Curve for the 24"/20W Fluorescent Tube.

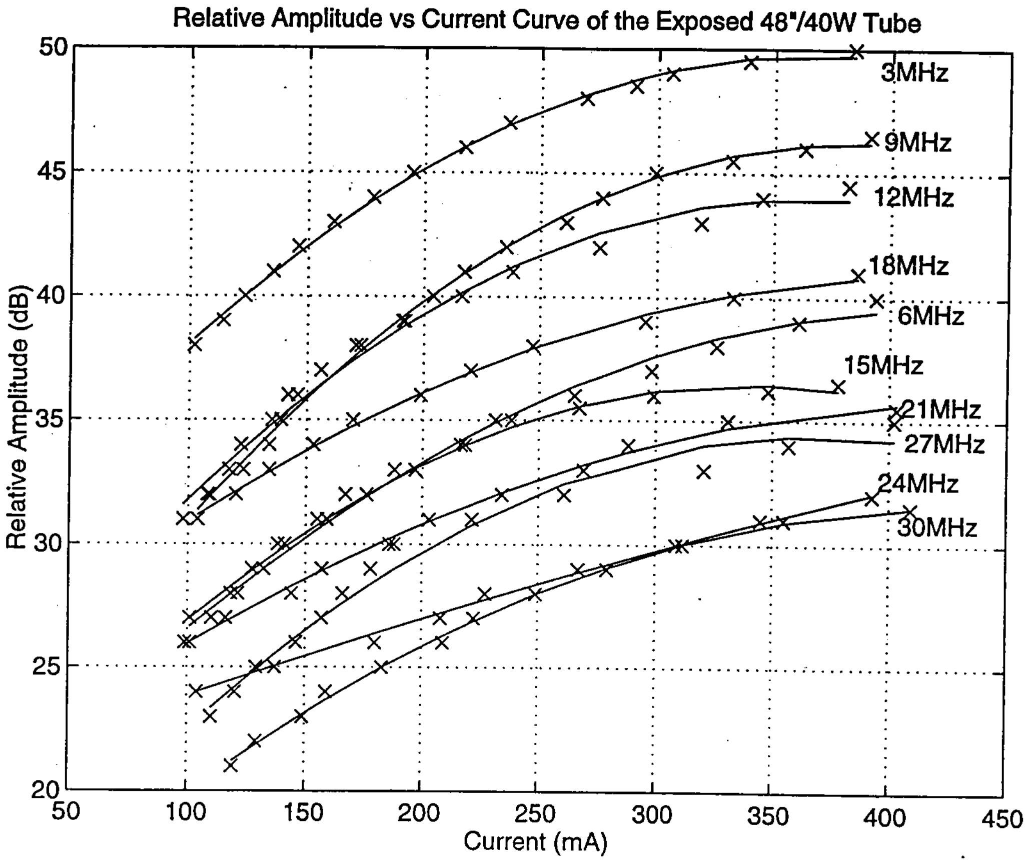

Figure 4.3 Relative Amplitude vs Current Curve for the Exposed 48"/40W Tube.

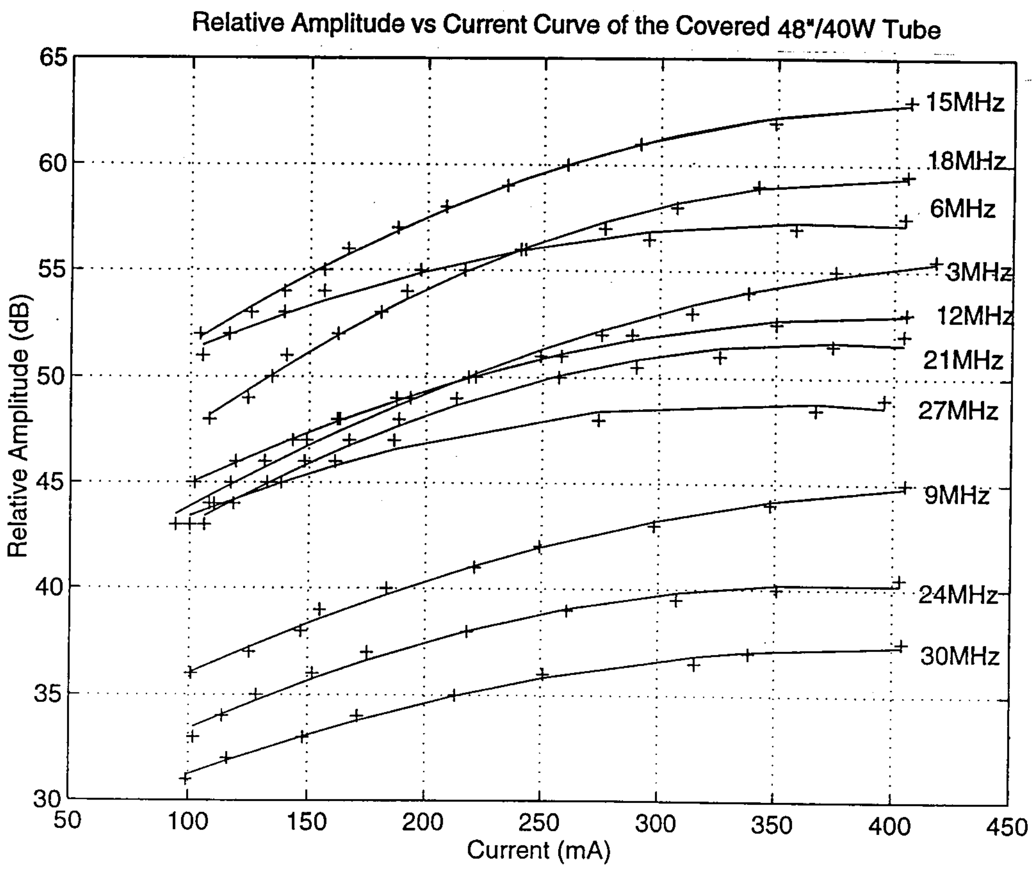

Figure 4.4 Relative Amplitude vs Current Curve for the Covered 48"/40W Tube.

by an outer conductor pipe. It is obvious that the tube with an outer conductor has a better relative amplitude gain. It thus enhances our assertion that the coaxial plasma line structure acts as an excellent conducting device that can efficiently transmit microwave.

The curve, however, does not reveal a clear-cut relationship between the relative amplitude and the transmitting frequency.

The similar relative amplitude versus current curves for the 24"/20W tube are shown in Figures 4.5 and 4.6, representing the tube that is exposed and covered respectively.

c) Relative Amplitude at Constant Current

For above 30 MHz signals, we did not measure the relative amplitude at various current intervals. Instead, we measured the relative amplitude only at the current of approximately 400 mA.

We thus present our results from Figure 4.7 to Figure 4.16. the relative amplitudes at various transmitting frequencies. On each of the figures presented, the upper curve represents the amplitude when the plasma is on and the lower curve when the gas is de-ionized. The value of the relative amplitude is also indicated in the figures.

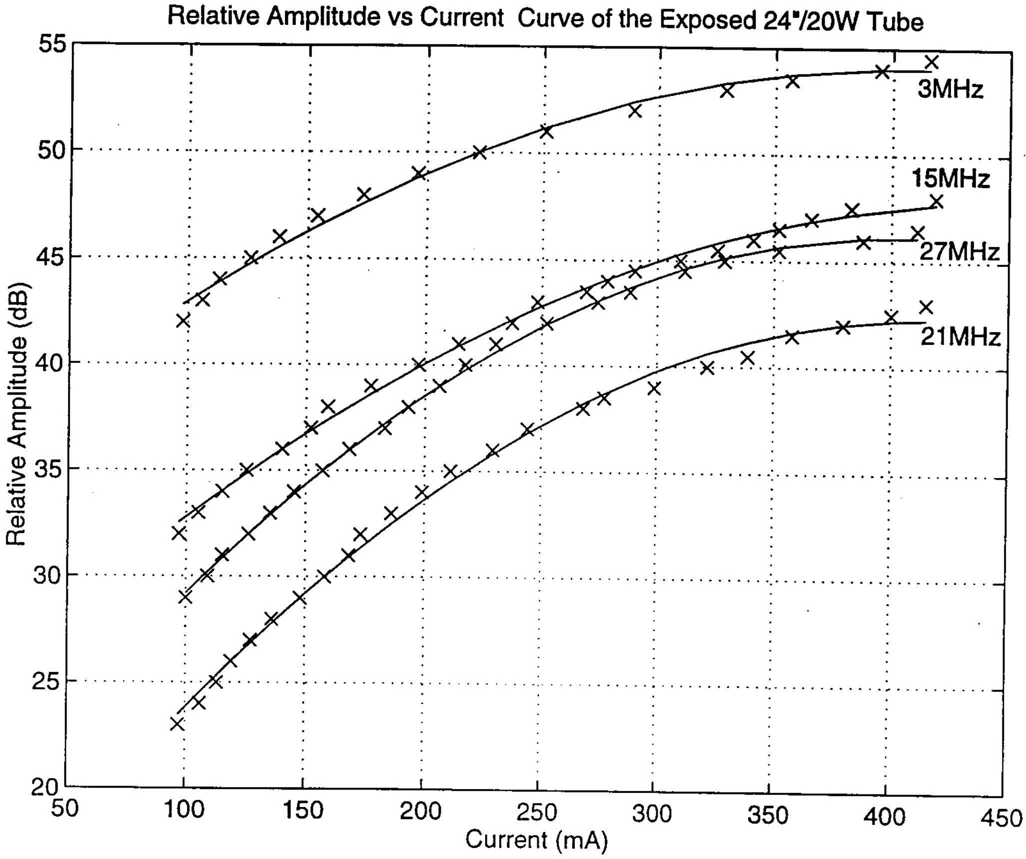

Figure 4.5 Relative Amplitude vs Current Curve for the Exposed 24"/20W Tube

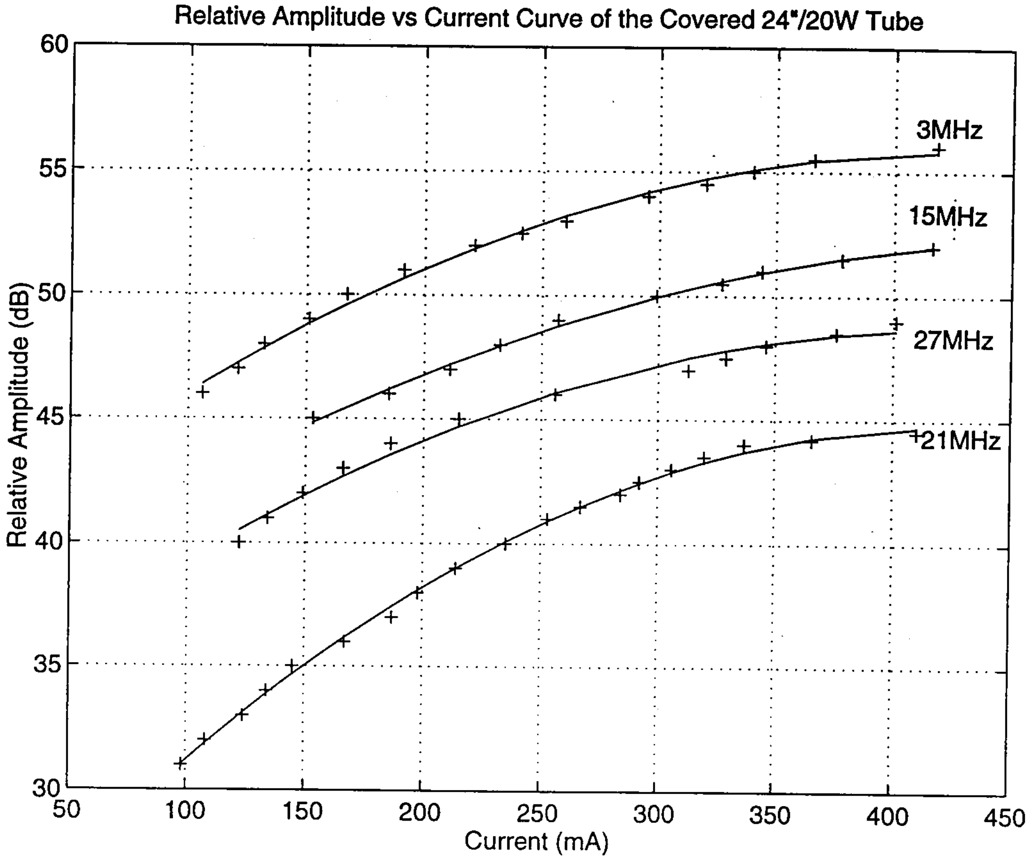

Figure 4.6 Relative Amplitude vs Current Curve for the Covered 24"/20W Tube

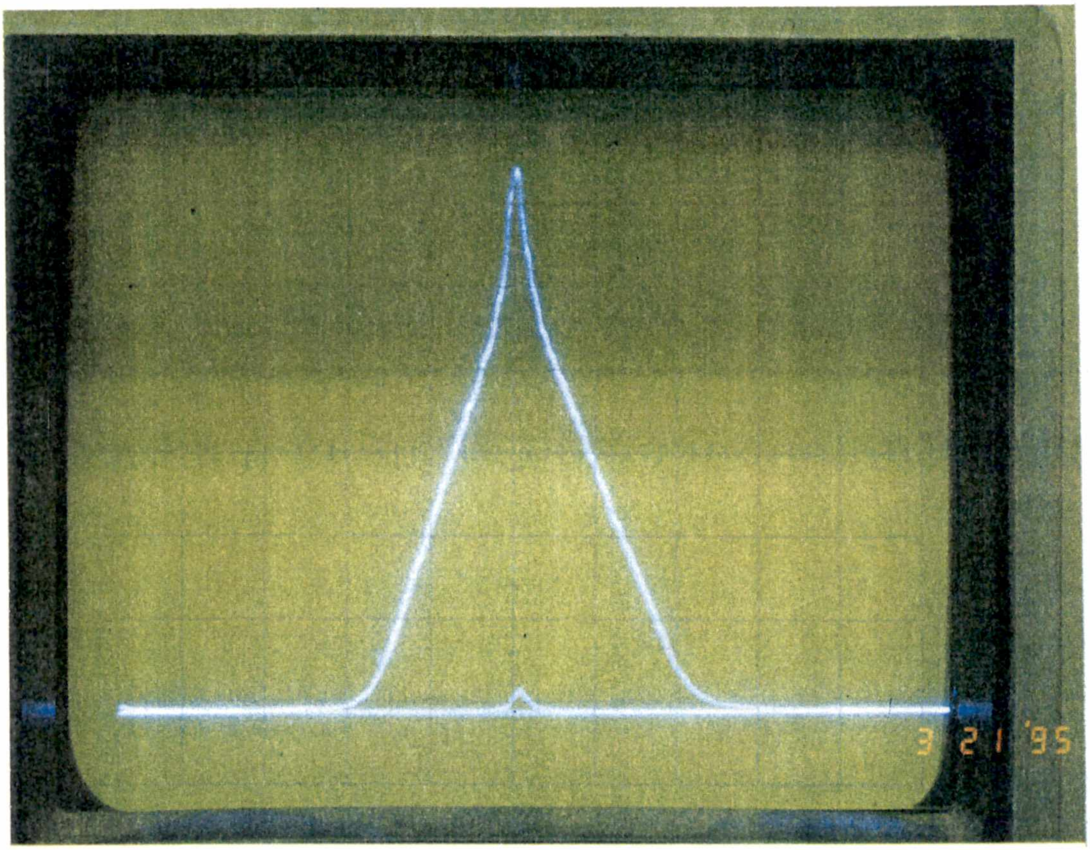

Figure 4.7 The Relative Amplitude of the 30 MHz Signal with Gain of 44 dB.

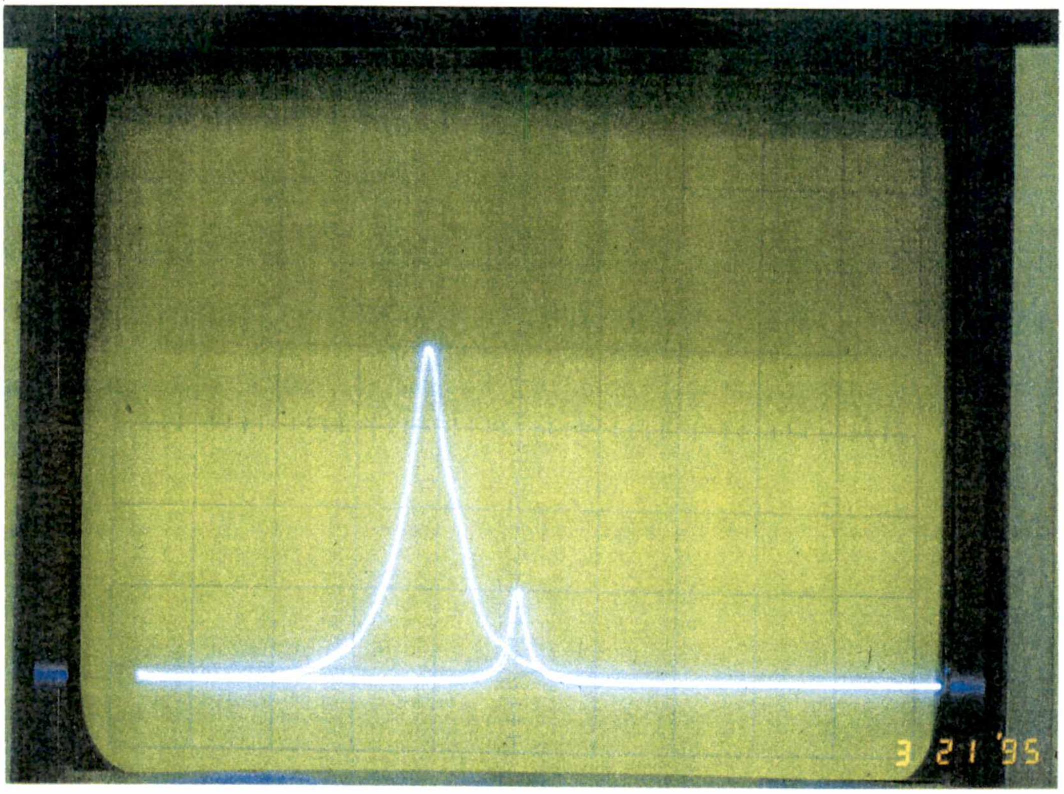

Figure 4.8 The Relative Amplitude of the 90 MHz Signal with Gain of 16 dB.

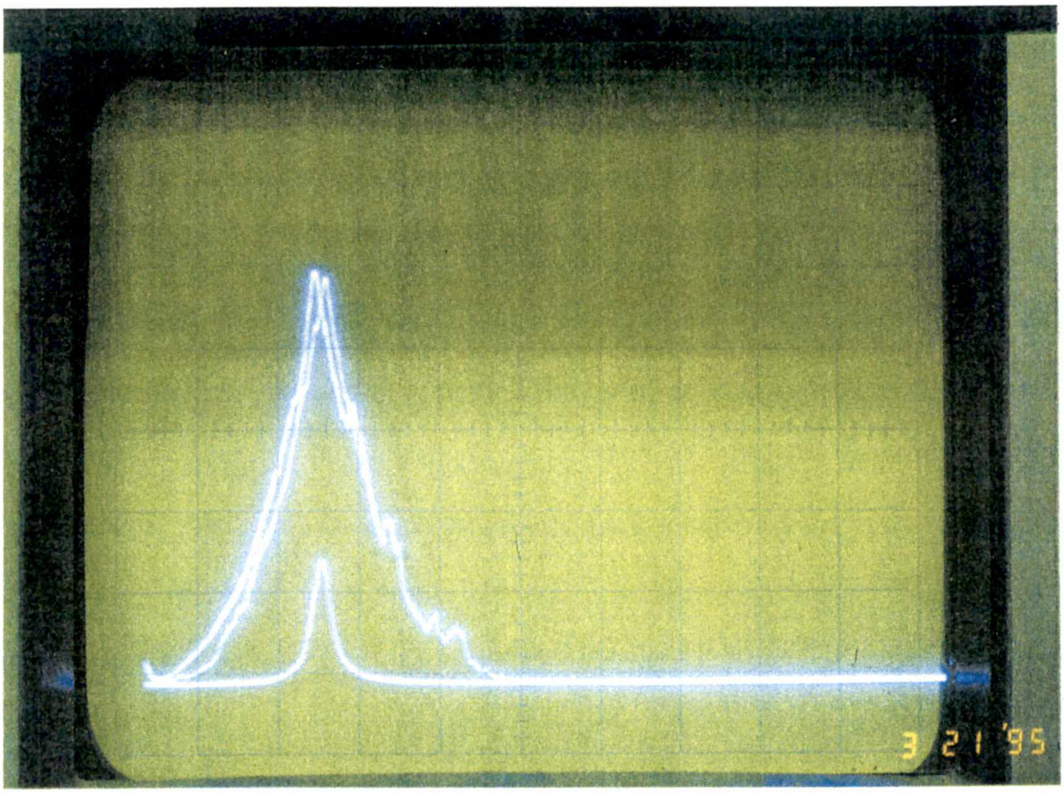

Figure 4.9 The Relative Amplitude of the 270 MHz Signal with Gain of 20 dB.

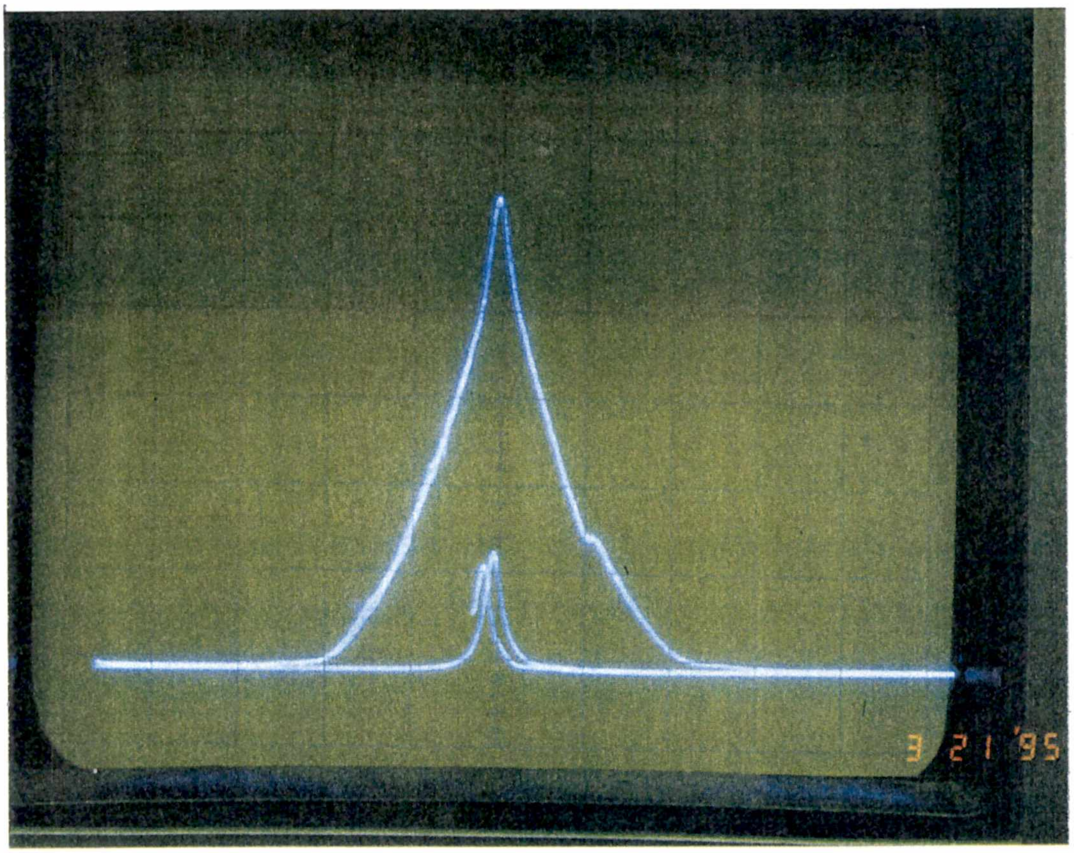

Figure 4.10 The Relative Amplitude of the 300 MHz Signal with Gain of 25 dB.

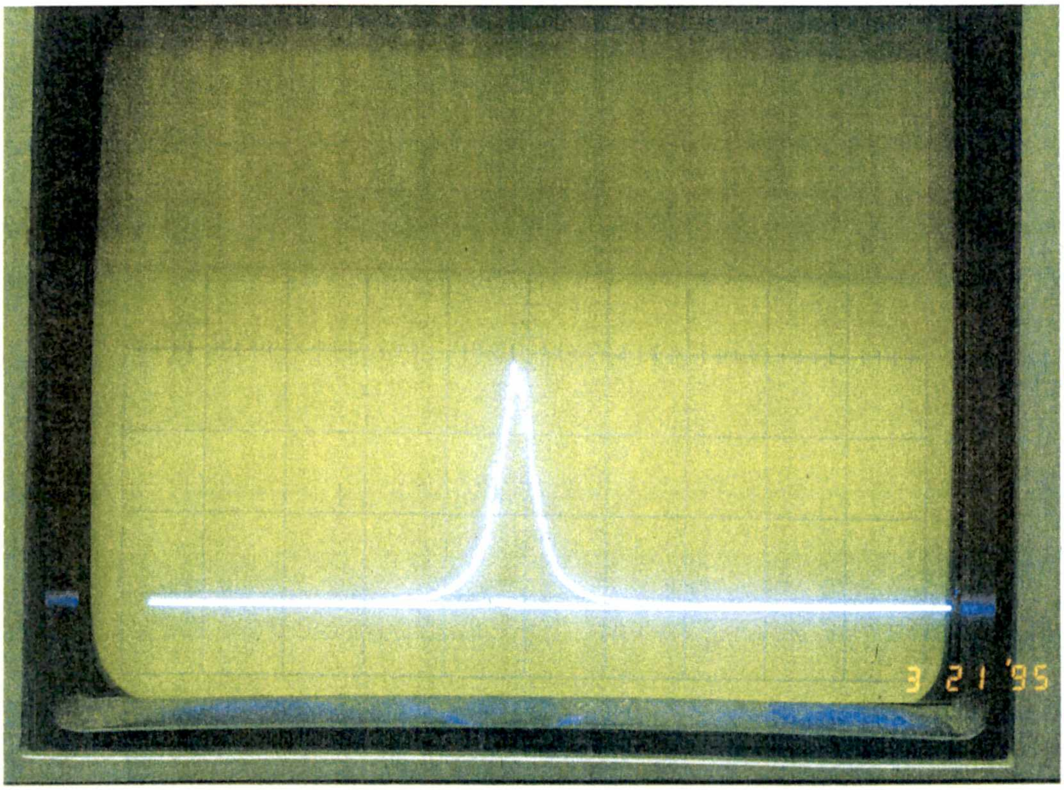

Figure 4.11 The Relative Amplitude of the 400 MHz Signal with Gain of 22 dB.

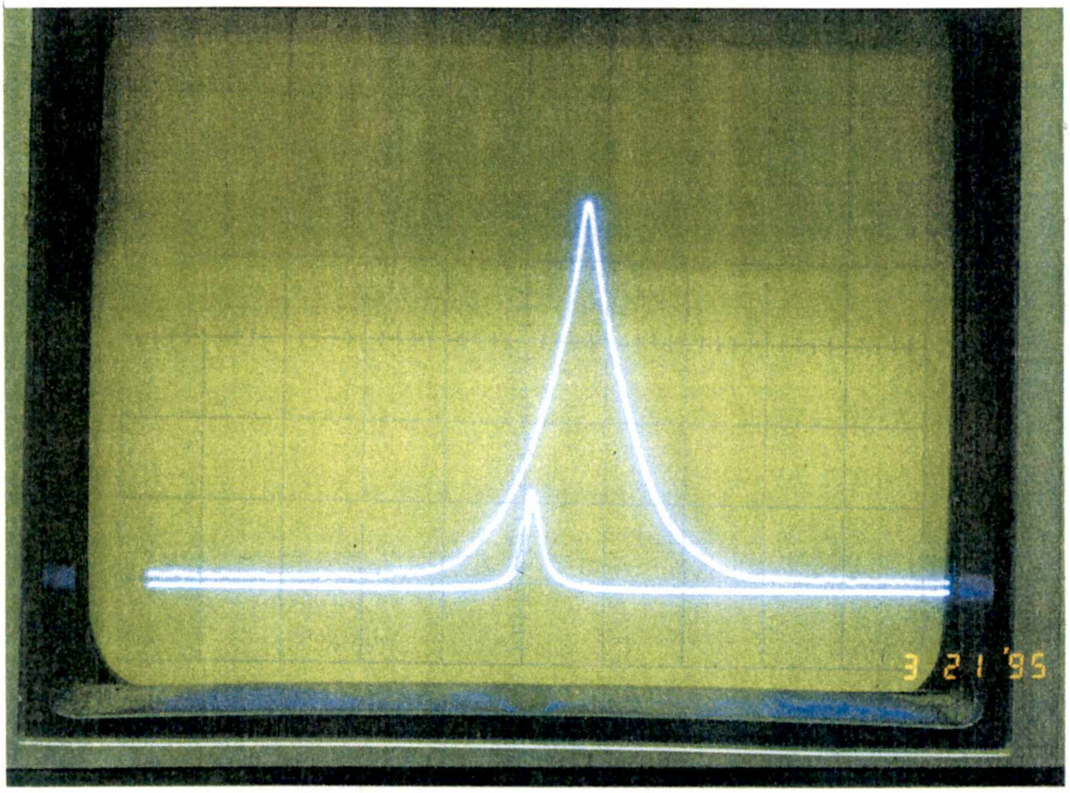

Figure 4.12 The Relative Amplitude of the 500 MHz Signal with Gain of 20 dB.

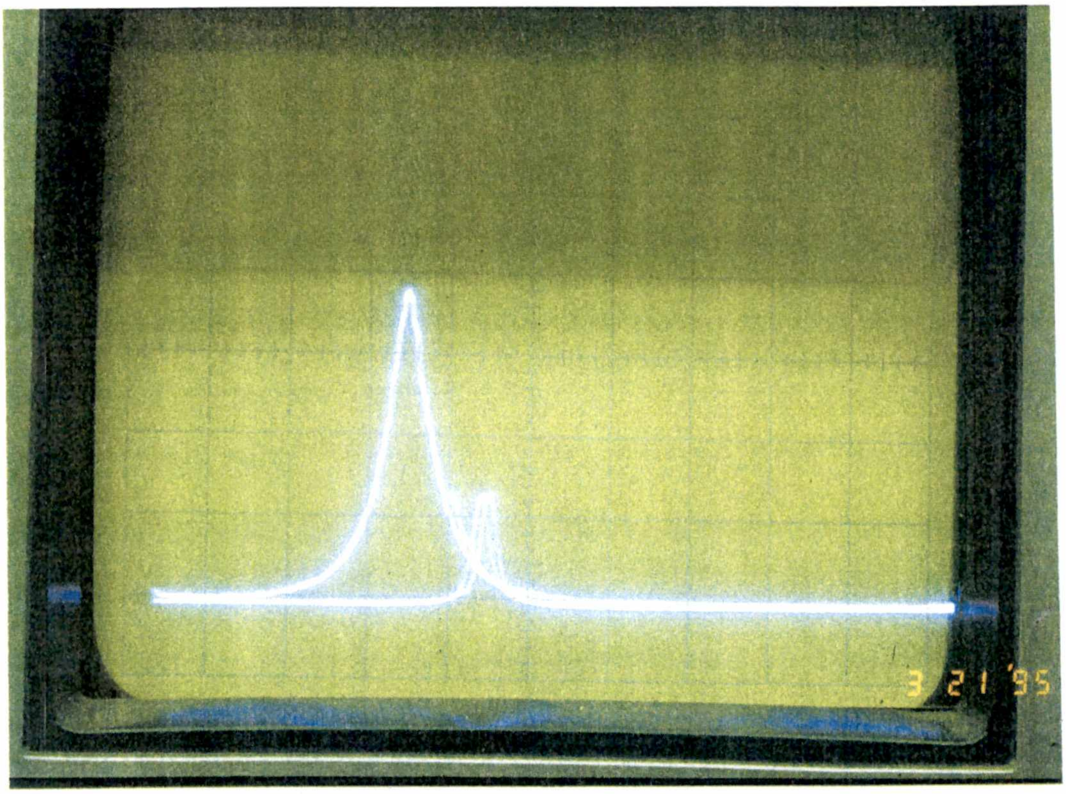

Figure 4.13 The Relative Amplitude of the 600 MHz Signal with Gain of 16 dB.

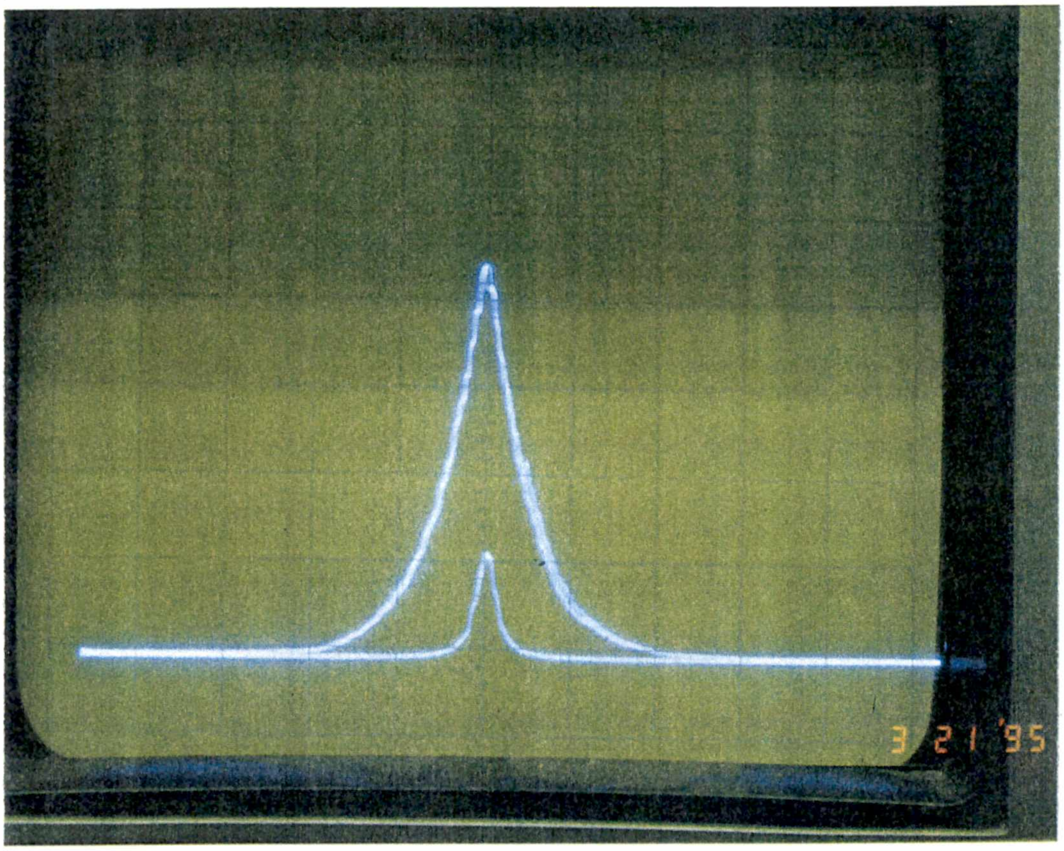

Figure 4.14 The Relative Amplitude of the 700 MHz Signal with Gain of 20 dB.

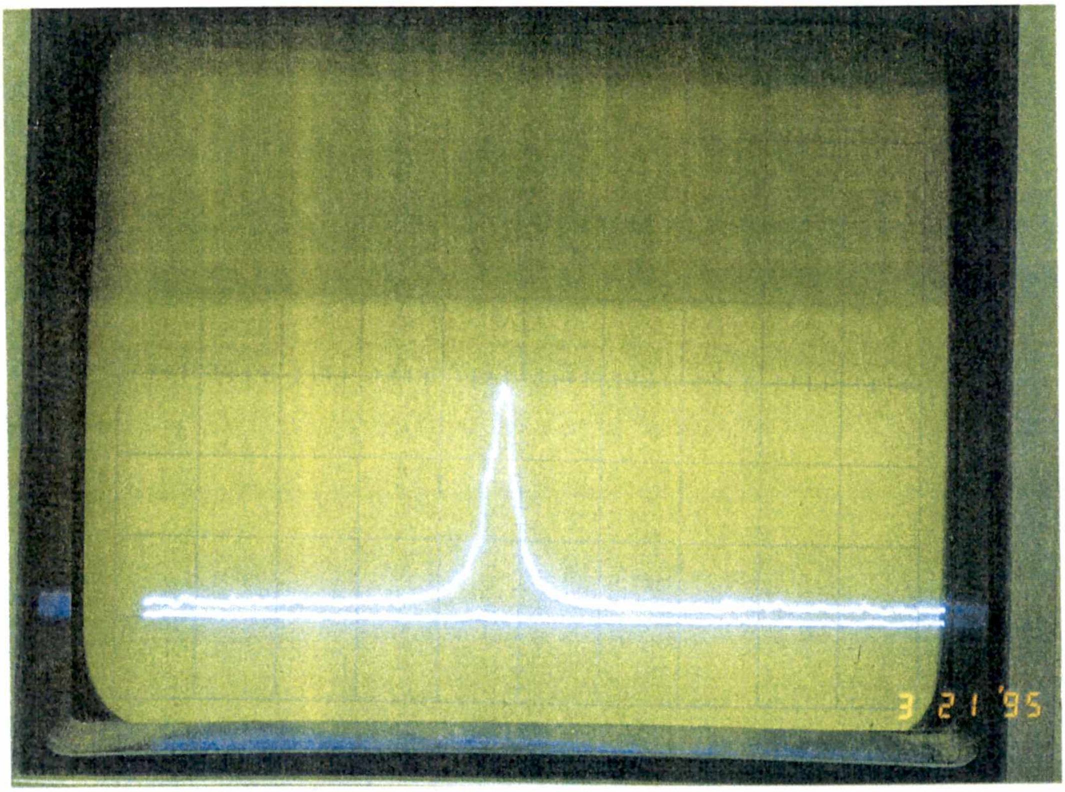

Figure 4.15 The Relative Amplitude of the 800 MHz Signal with Gain of 20 dB

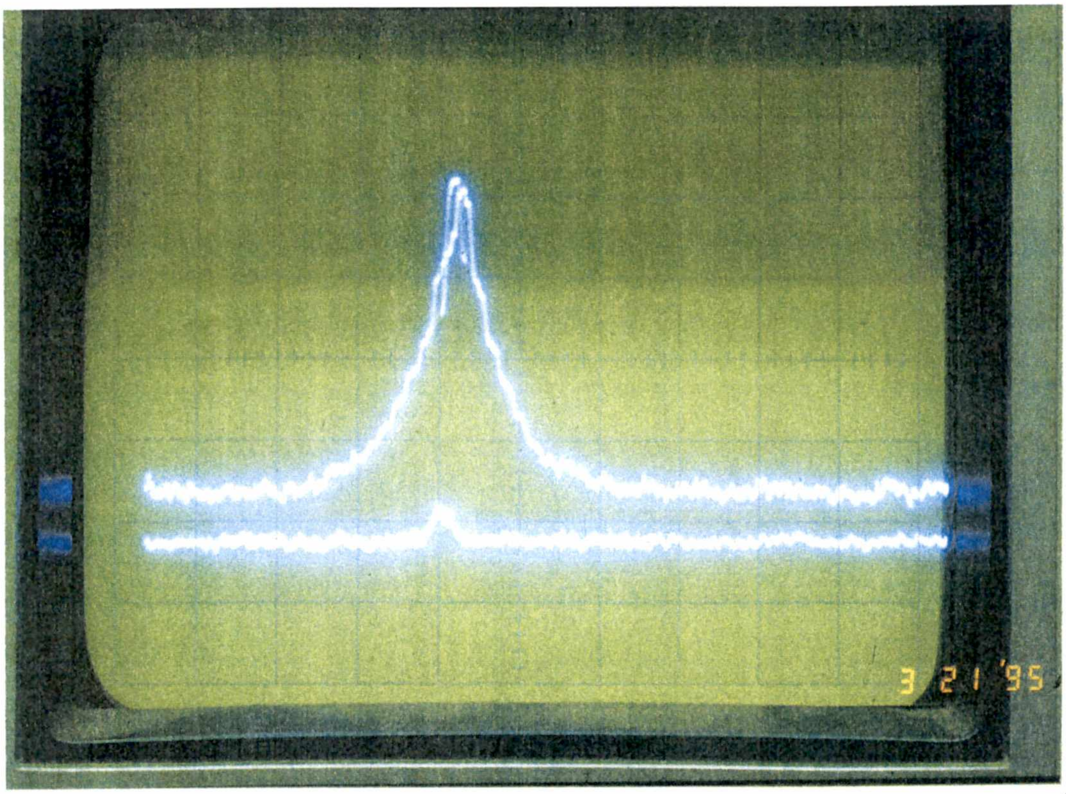

Figure 4.16 The Relative Amplitude of the 900 MHz Signal with Gain of 21 dB.

In most of the cases, we have obtained a relative amplitude beyond 20 dB. Even at the 900 MHz frequency, we still achieved a relative amplitude of 21 dB. However, we were unable to obtain a reliable or noticeable relative amplitude in the GHz range. This is probably due to the limitation of the plasma density attained by our 24"/20W fluorescent tube. The plasma density of a typical fluorescent tube is approximately 10^{16} electron/m^3 .

Chapter 5

THEORETICAL AND EXPERIMENTAL FIT

a) Theoretical Evaluation for V/V_o

We have found in Equation (2.40), an expression for V , namely

$$V = V_0 e^{-\frac{a L_t i_{av}}{2\sqrt{L_0/C_0}\, i}} \tag{5.1}$$

We now try to find the numerical values for L_o, C_o, and a. From equations (2.21) and (2.24), we can express

$$L_0/C_0 = \frac{\mu_0}{4\pi^2\varepsilon_0}[\ln(b/a)]^2 \tag{5.2}$$

Thus

$$\sqrt{L_0/C_0} = \frac{1}{2\pi}\sqrt{\frac{\mu_0}{\varepsilon_0}}\ln(b/a) \tag{5.3}$$

By using μ_0=1.26x10^{-6} henry/meter and ε_o =8.85x10^{-12} farad/meter, and the fact that ln(b/a)≈1 for our coaxial line system, equation (5.3) becomes

$$\sqrt{L_0/C_0} = 60\Omega \tag{5.4}$$

To find the voltage drop per unit length a , we use the numerical values for the 48" and 24" tubes we found in the experiment.

For the 48" tubes, the average voltage and current are 111.06 volts and 219.4 mA respectively, while that for the 24" tube are 58.53 volt and 314.67 mA respectively.

Thus, we can form the following equations

$$116.06 = 48a + b \tag{5.5a}$$

$$58.53 = 24a + b \tag{5.5b}$$

where a is the voltage drop per inch and b is the cathode voltage drop.

Solving equations (5.5a) and (5.5b), we found that

$$a = 2.19 volt / inch \ = 86.1713 volt / meter \tag{5.6}$$

Substituting (5.4) and (5.6) into equation (5.1), we get

$$V = V_0 e^{-\frac{0.7181 L_t i_{av}}{i}} \tag{5.7}$$

For the 48" tube with i_{av} = 219.4, equation (5.7) becomes

$$V = V_0 e^{-\frac{0.1921}{i}} \tag{5.8}$$

For the 24" tube with i_{av} = 314.67, equation (5.7) becomes

$$V = V_0 e^{-\frac{0.1377}{i}} \tag{5.9}$$

b) Theoretical and Experimental Fit

The relative amplitude measurement is the measurement of energy, thus from equations (5.8) and (5.9) we get

$$(V/V_o)^2 = e^{-0.3842/i} \qquad (5.10)$$

$$(V/V_o)^2 = e^{-0.2754/i} \qquad (5.11)$$

To compare the theoretical prediction of equation (5.10), with experimental values for the 3 MHz signal, Table 5.1 is presented. The first and second columns are the experimental values. Column 3 is the prediction of equation (5.10) using current values of column one.

Column four is the correction factor, representing the difference between column two and three. We found that the correction is almost a constant, with an average value of 58.1543 dB.

Column five is the value representing the sum of the average correction factor and column three. Surprisingly, the resulting value is very close to the experimental values shown in column two.

The relative amplitude plot for column two is shown in Figure 5.1, using the 4th degree polyfit function[5.1] found in MATLAB[5.2], while that for column three is shown in Figure 5.2. Figure 5.3 is the plot of column two, three, and five altogether, revealing the closeness between theoretical and experimental values.

Table 5.1 Theoretical and Experimental Comparison of the Relative Amplitude for the 3 MHz Signal in the 48" Fluorescent Tube.

Current (mA)	Experimental Relative Amplitude (dB)	$(\frac{V}{V_0})^2 = e^{-\frac{0.3842}{i}}$ (dB)	Correction Factor	Final Theoretical Relative Amplitude (dB)
95	42	-17.5638	59.5638	40.5905
106	43	-15.7411	58.7411	42.4132
113	44	-14.7660	58.7660	43.3883
126	45	-13.2425	58.2425	44.9118
138	46	-12.0910	58.0910	46.0633
154	47	-10.8348	57.8348	47.3195
173	48	-9.6449	57.6449	48.5094
196	49	-8.5131	57.5131	49.6412
222	50	-7.5160	57.5160	50.6383
251	51	-6.6476	57.6476	51.5167
289	52	-5.7736	57.7736	52.3807
329	53	-5.0716	58.0716	53.0827
357	53.5	-4.6738	58.1738	53.4805
395	54	-4.2242	58.2242	53.9301
416	54.5	-4.0110	58.5110	54.1430
			average 58.1543	

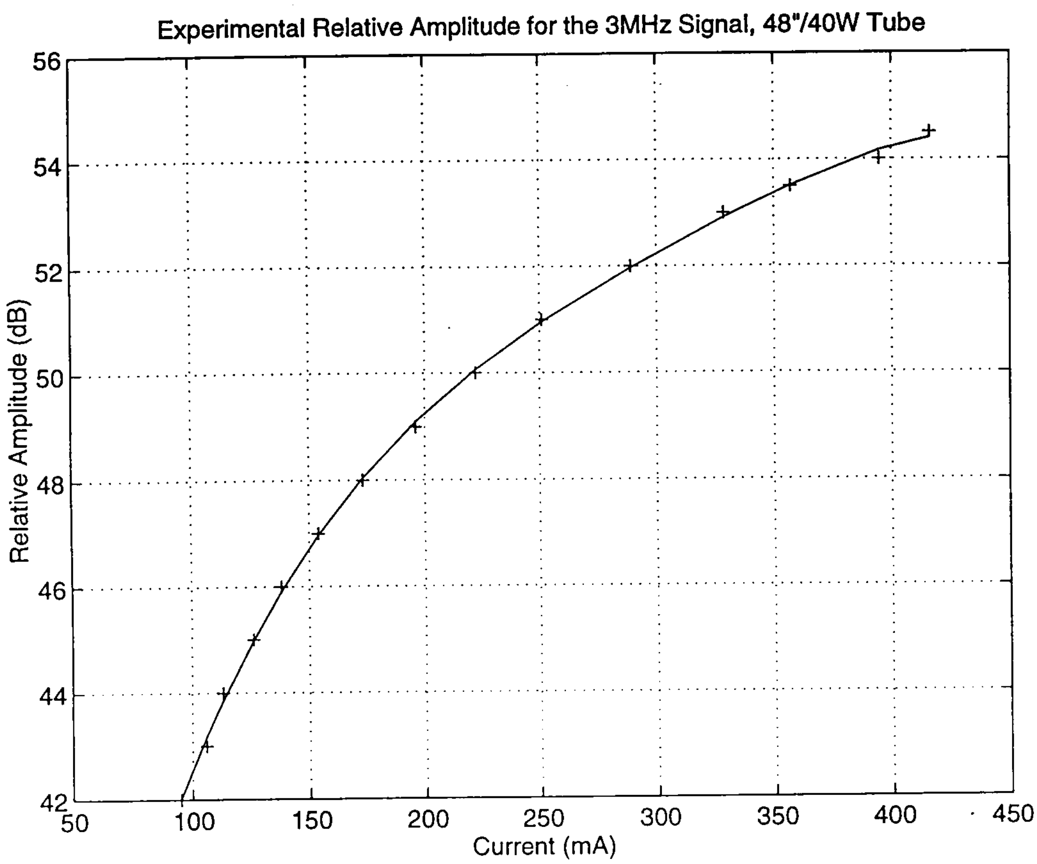

Figure 5.1 Experimental Relative Amplitude for the 3 MHz Signal Transmitting Through the 48"/40W Tube.

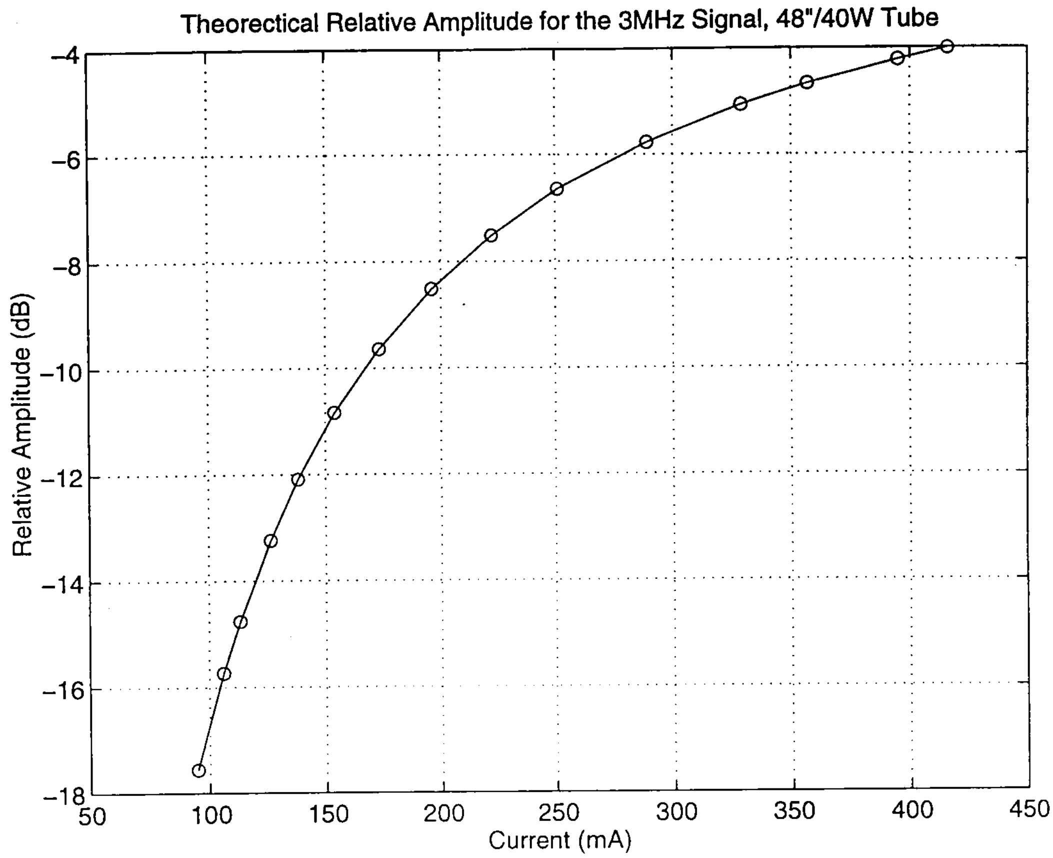

Figure 5.2 Theoretical Relative Amplitude for the 3 MHz Signal Transmitting Through the 48"/40W Tube.

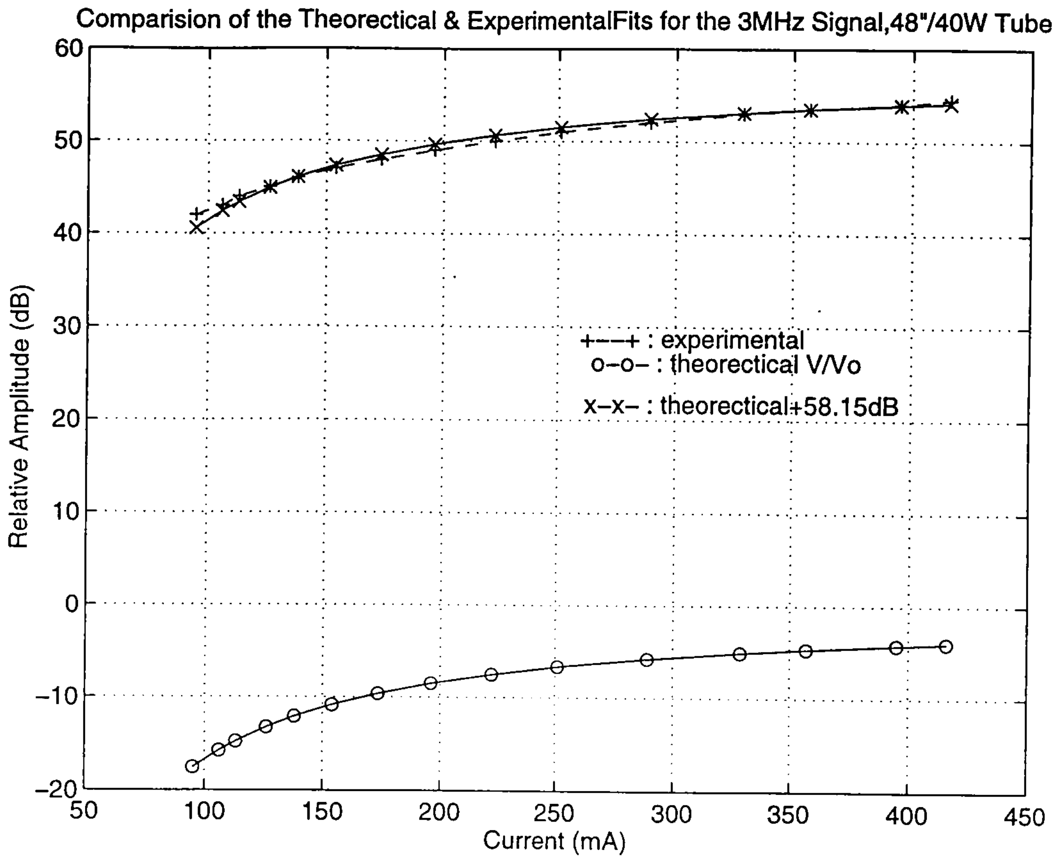

Figure 5.3 Theoretical and Experimental Fit for the 3 MHz Signal Transmitting Through the 48"/40W Tube.

We do the same analysis for the 3 MHz signal transmitting through the 24"/20W tube. The result is presented in Table 5.2 and Figures 5.4, 5.5, and 5.6. The correction factor is 57.68 dB.

The approximately 58 dB correction factor is the Von/Voff ratio. The off value is due to the microwave leakage, which is a constant and is not covered in our theory.

c) Collision Frequency

We have assumed in our work that the collision frequency v_c is greater than the transmitting wave frequency ω. We now proceed to calculate the collision frequency.

The collision frequency is that of the electron neutral collision and can be expressed as [5.3]

$$v_c = 2.8x10^8[r_n(cm)]^2[n_n(cm^{-3})][T_e(eV)]^{1/2} \qquad (5.12)$$

where r_n is the effective radius of the neutral, n_n the neutral density, and T_e the electron temperature.

A typical fluorescent tube contains argon at a pressure of a few mmHg for starting[5.4] , together with a small drop of mercury. Thus, if we assume a pressure of 4 torr, and a temperature of 300 ^{0}k, the neutral density can be evaluated from the ideal gas law[5.5]

Table 5.2 Theoretical and Experimental comparison of the Relative Amplitude for the 3 MHz Signal in the 24 " Tube

Current (mA)	Experimental Relative Amplitude (dB)	$(\frac{V}{V_0})^2 = e^{\frac{0.2754}{i}}$ (dB)	Correction Factor (dB)	Final Theoretical Relative Amplitude (dB)
106	46	-11.2876	57.2876	46.3923
121	47	-9.8883	56.8883	47.7916
132	48	-9.0643	57.0643	48.6156
151	49	-7.9237	56.9237	49.7562
167	50	-7.1646	57.1646	50.5153
191	51	-6.2643	57.2643	51.4156
221	52	-5.4139	57.4139	52.0813
241	52.5	-4.9647	57.4647	52.7152
260	53	-4.6019	57.6019	53.0780
295	54	-4.0559	58.0559	53.6240
320	54.5	-3.7390	58.2390	53.9401
340	55	-3.5191	58.5192	54.1608
366	55.5	-3.2691	58.7691	54.4108
418	56	-2.8624	58.8624	54.8175
			average 57.6799	

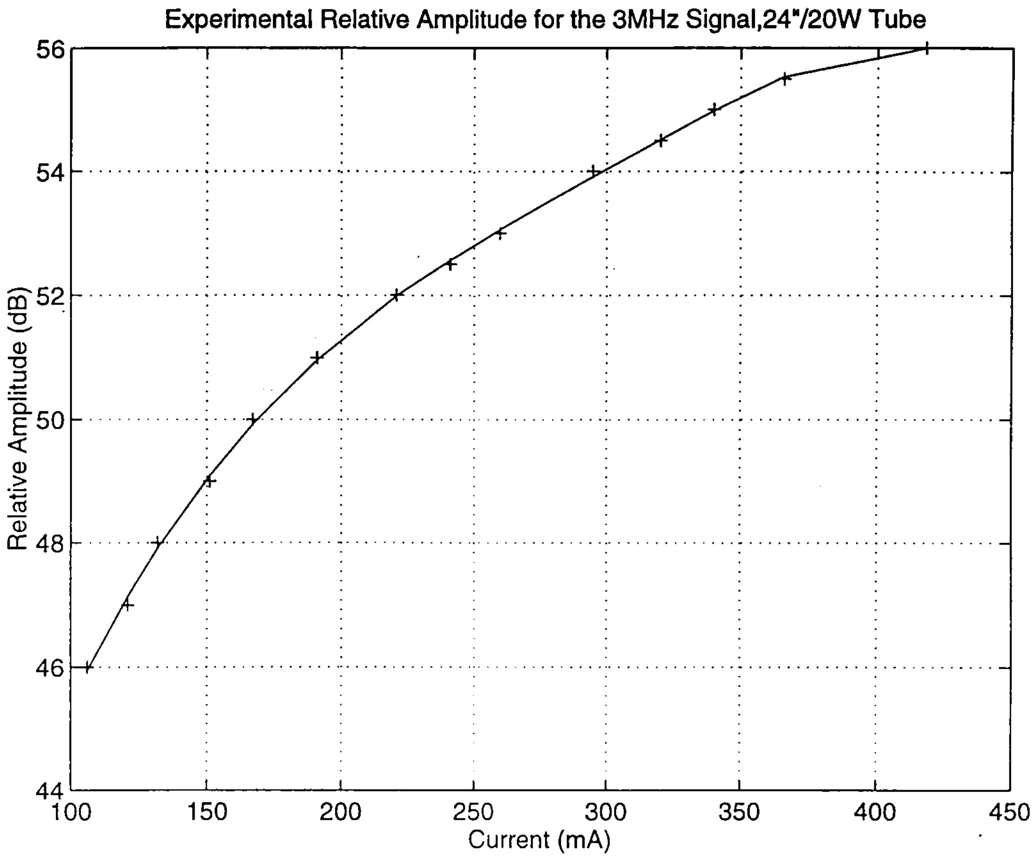

Figure 5.4 Experimental Relative Amplitude for the 3 MHz Signal Transmitting Through the 24"/20W Tube.

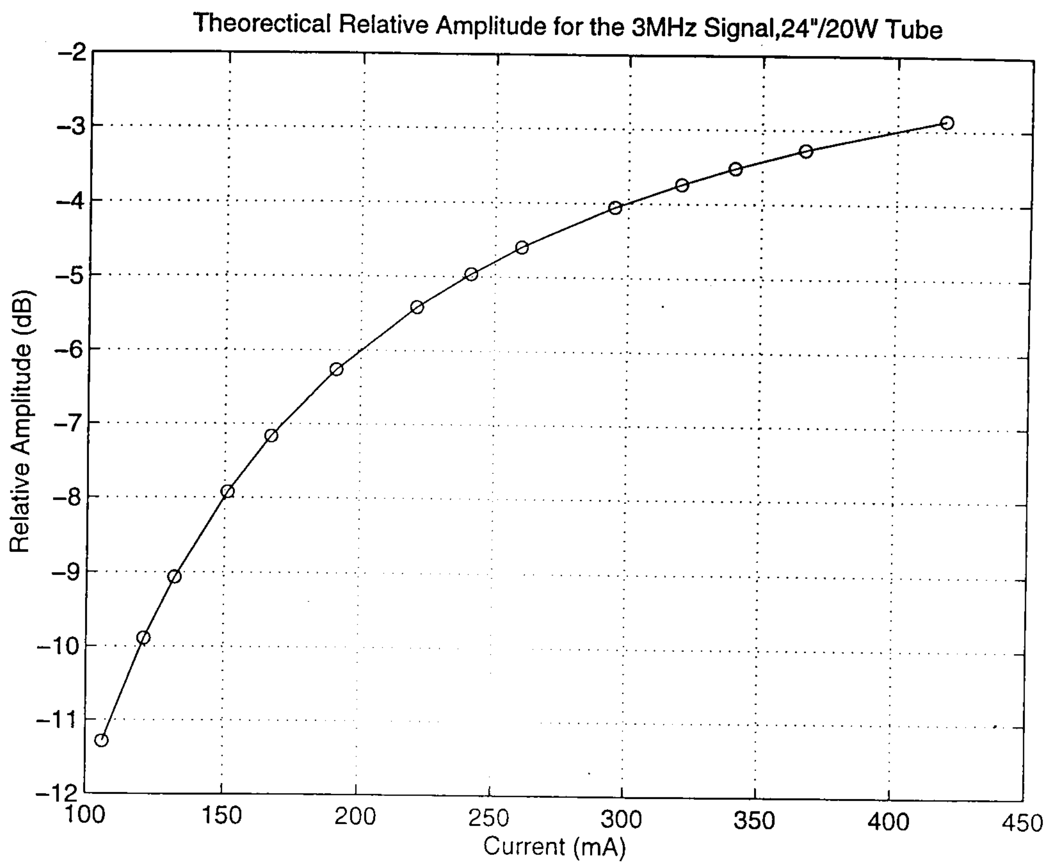

Figure 5.5 Theoretical Relative Amplitude for the 3 MHz Signal Transmitting Through the 24"/20W Tube.

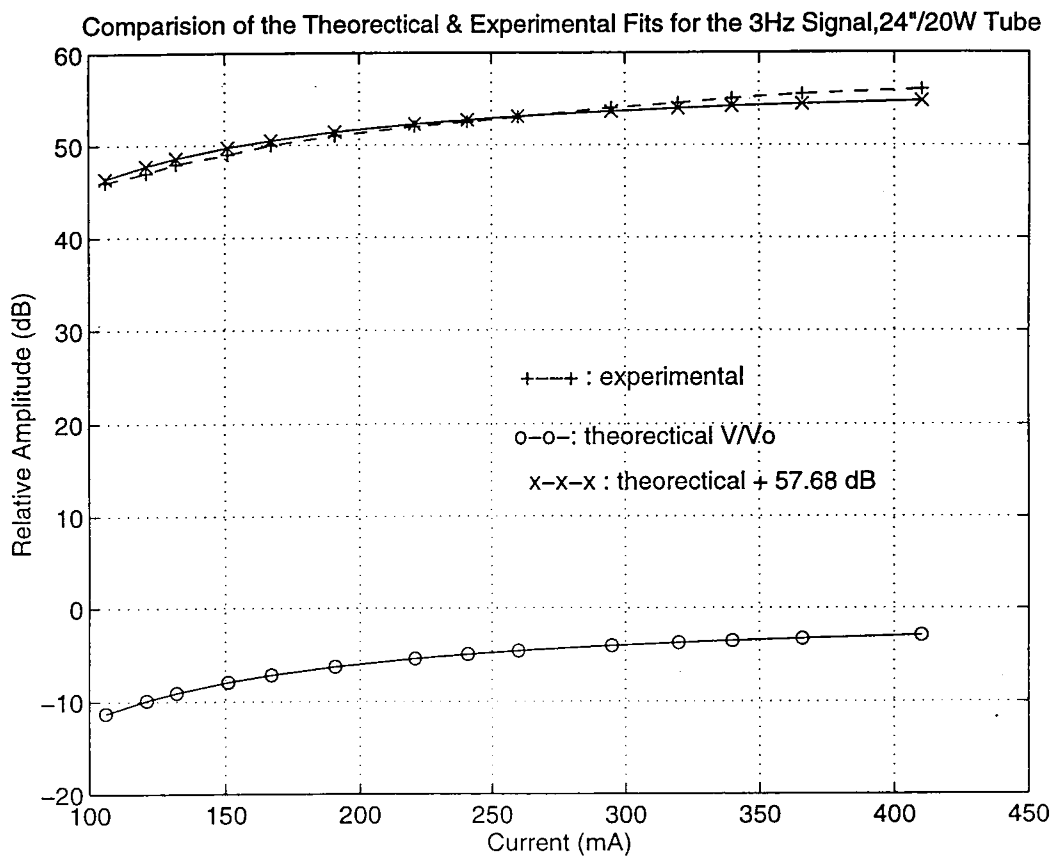

Figure 5.6 Theoretical and Experimental Fit for the 3 MHz Signal Transmitting Through the 24"/20W Tube.

$$n_n = \frac{p}{kT}$$
$$= 3.22x10^{22}[p(torr)]$$
$$= 1.29x10^{23} atoms / m^3 \qquad (5.13)$$

The effective radius r_n of argon atom is approximately 1.82x10-8 cm [5.6], whereas a typical Te for a fluorescent tube is about 2 ev[5.7]. Thus ν_c can be estimated from equation (5.12) to be

$$\nu_c = 1.69x10^{10} collision / \sec \qquad (5.14)$$

This collision frequency is greater than the transmitting wave frequencies used in our work.

Chapter 6

STEALTH PLASMA ANTENNA

a) The Plasma Cloaking Effect

The United States Department of Defense has always been interested in using an ionized gas, or a plasma, to absorb or modify radar signal, thus rendering a radar cloaking effect. The University of Tennessee Plasma Science Laboratory, supporting by the AFOSR , has successfully demonstrated that cloaking effects can actually be achieved by plasma-induced frequency shifts in microwave beams[6.1]. Such a frequency shifting system achieves the stealth effect by changing the frequency of a radar signal to move it out of the pass band of a radar system.

The stealth plasma antenna, to be discussed in the following sections and chapters, does not achieve stealth effect based on frequency shifting. It bases its working principles on the behavior of an electromagnetic wave propagating in a plasma medium.

b) Effects of Electron Plasma Frequency

How an electromagnetic wave propagates in a plasma medium depends largely on a very important plasma parameter known as the electron plasma frequency. It is the frequency with which the electrons oscillate among the heavier, immobile ions when the electrons are disturbed.

The electron plasma frequency f_{pe} can be defined [6.2] as

$$f_{pe} = \frac{\omega_{pe}}{2\pi} = 8.98x10^3\sqrt{n_e} \qquad (6.1)$$

where

$$\omega_{pe} = \sqrt{\frac{4\pi n_e e^2}{m}} \qquad (6.2)$$

Note that equations (6.1), and (6.2) are in cgs units. In the SI units, these equations become

$$f_{pe} = 8.98\sqrt{n_e} \qquad (6.3)$$

and

$$\omega = \sqrt{\frac{n_e e^2}{m\varepsilon_0}} \qquad (6.4)$$

Now if the electromagnetic radiation is incident on the plasma with a frequency f less than the electron plasma frequency f_{pe} , the individual electron at the surface of the plasma will act like miniature dipoles and re-radiate the incident radiation, reflecting it from the plasma[6.3].

If the incident radiation has a frequency f greater than the electron plasma frequency f_{pe} , the electrons have too much inertia to respond to the electric field of the wave, and the radiation is able to propagate through the plasma without reflection or attenuation[6.4].

The description in the last two paragraphs can be depicted in Figure 6.1.

c) Basic Idea Behind the Stealth Plasma Antenna

The basic incentive of constructing a stealth plasma antenna is that a plasma system can be turned on and off rather easily.

When the gas in the antenna is ionized and if the electron plasma frequency is less than the incident radar frequency, the antenna achieves its stealth effect without any difficulty. This is because the wave will propagate through the plasma as described in the previous section. No reflection is expected in this case.

Now if the electron plasma frequency is greater than the incident radar frequency, what would happen ? One would expect that the wave will be reflected and thus picked up by the radar detection. However, since the gas can be de-ionized instantly, the radar cross section would be negligible, rendering the plasma antenna a stealth property.

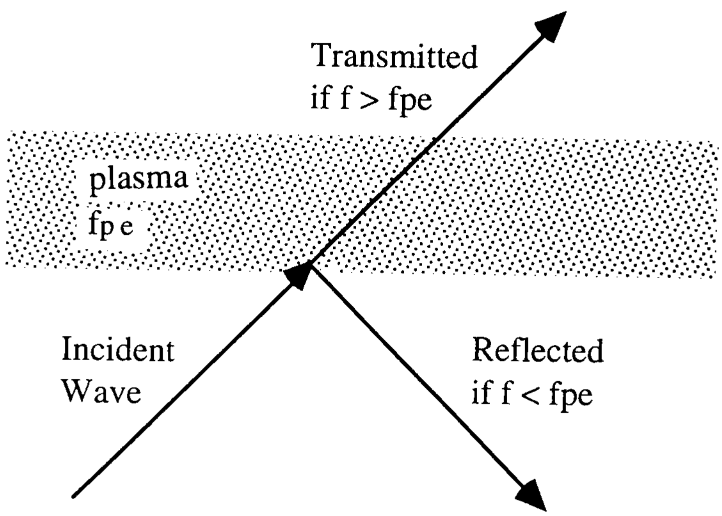

Figure 6.1 Electromagnetic Wave Propagation in a Plasma Medium.

Chapter 7

STEALTH PLASMA ANTENNA EXPERIMENT

a) Experimental Set-up

The schematic of the experimental set-up is shown in Figure 7.1. The fluorescent tube acts as a reflector. The spark gaps are for creating a pulse signal through the tube. The plasma density created by such a circuit is usually two orders higher than the usual density of 10^{16} electrons/m^3.

The elements of the circuit include:-

1) a VARO dc power supply capable of producing 13.5kV peak at 0.31 mA.

2) a resistor of 1 kΩ

3) a Faradon capacitor with capacitance of 0.004μF, effective voltage of 3 kv, a current of 5.5 amperes, and a frequency of 300 kilo cycles.

4) a Sylvania 8 watt cool white fluorescent tube (15" in length and 1" in diameter)

5) a transmitting horn connected to a 3.9 GHz transmitter

6) a receiving horn connected to a Tektronix 555 dual beam oscilloscope or 7503 oscilloscope.

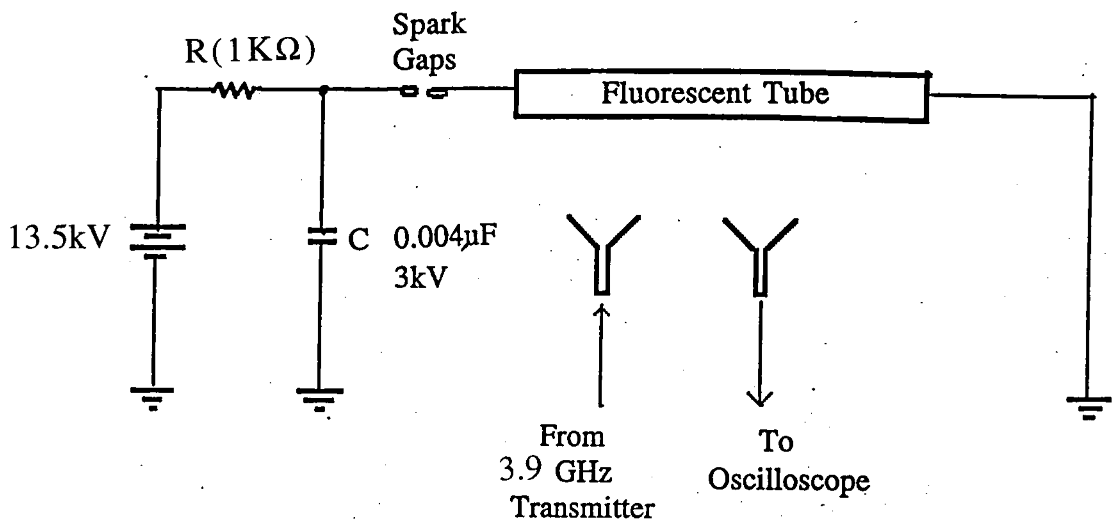

Figure 7.1 Schematic of Stealth Plasma Antenna.

b) Estimation of Electron Plasma Frequency

The plasma density is related to the current density j by the equation [7.1]

$$j = \frac{i}{A} = n_e e v \qquad (7.1)$$

where i is the current through the tube with a cross section area A, and v is the drift velocity.

The current is that created by the discharging capacitor, and can be estimated if we know the total charge Q stored in the capacitor and the charged time t of the capacitor. Thus, we have

$$\begin{aligned} Q &= CV \\ &\approx 0.004x10^{-6}x13.5x10^{3} \\ &= 54x10^{-6} coulomb \qquad (7.2) \end{aligned}$$

and

$$\begin{aligned} i &= \frac{\Delta Q}{\Delta t} \\ &\approx \frac{Q}{t} \\ &= 18 ampere \qquad (\text{ assuming } t=3\ \mu\text{sec}) \qquad (7.3) \end{aligned}$$

The cross section area A of the 1" diameter tube is $3.24x10^{-4}\ m^2$ where 0.4" radius has been used after the reduction of the thickness of the glass tube.

The Thermal velocity is estimated as

$$v = \sqrt{\frac{kT_e}{m}} = 4.19x10^5 m / \sec \qquad (7.4)$$

where 1 eV of thermal energy is estimated in the tube.

If we substitute the values of i , A , and v into equation (7.1) , we can get an estimated electron density n_e

$$n_e = \frac{i}{Aev} = 8.29x10^{17} electron / m^3 \qquad (7.5)$$

The corresponding electron plasma frequency f_{pe} can be estimated by using equation (6.4), namely

$$f_{pe} = 8.98\sqrt{n_e} = 8.17GHz \qquad (7.6)$$

Thus, an incident radiation with frequency f less than f_{pe} should be reflected from the tube.

c) Experimental Procedure

The equipment set-up has already been described in section a) and depicted in Figure 7.1. The photo of the equipment set-up is shown in Figure 7.2 which is self-explanatory.

In order to detect any reflected signal, the receiving horn must be placed along the path of the reflected beam. This can be done by placing the receiving horn on top of the transmitting horn as shown in Figure 7.3. To receive the best

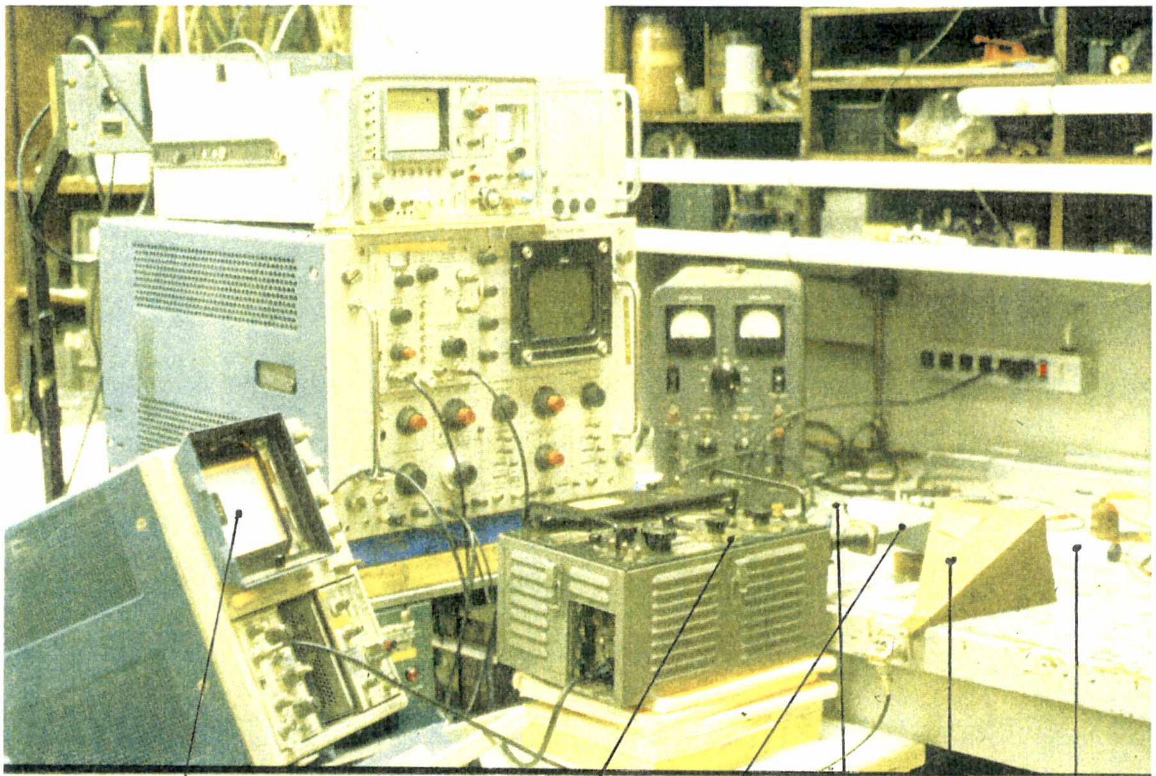

Figure 7.2 Equipment Set-up for the Stealth Plasma Antenna.

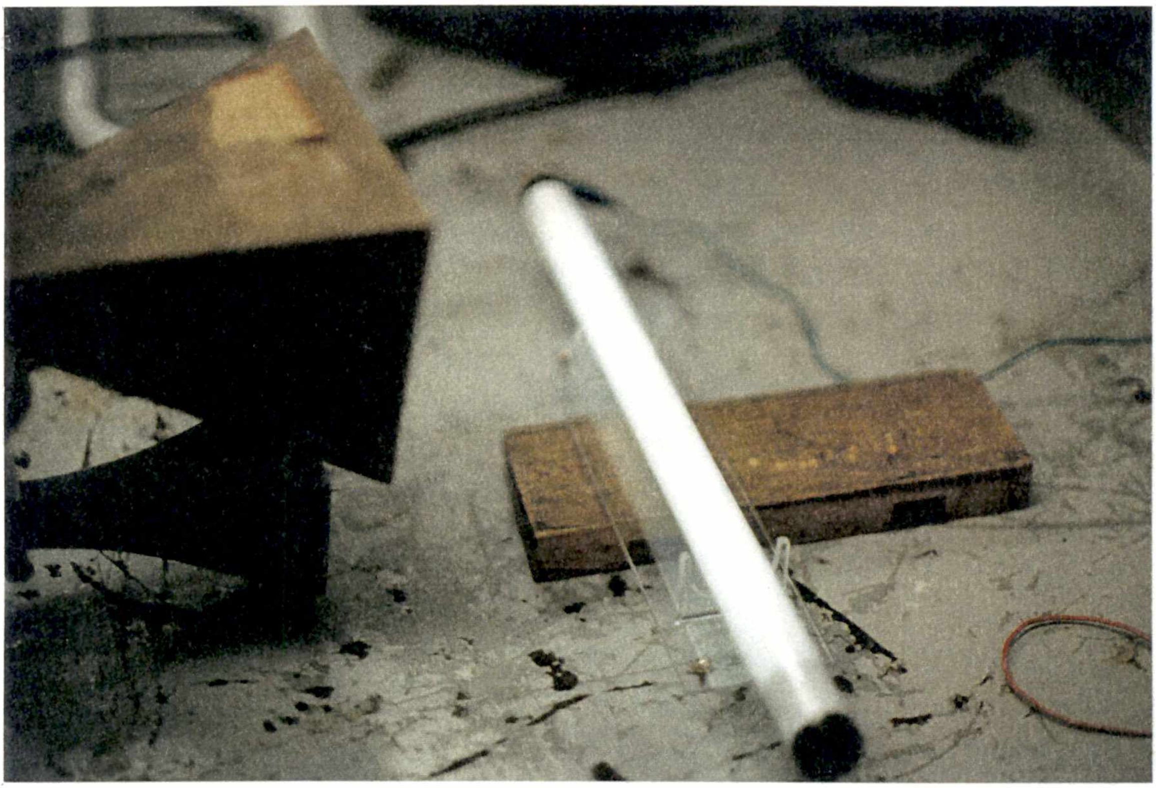

Figure 7.3 Position of the Receiving Horn along the Path of the Reflecting Beam.

of the reflected signal, the receiving horn has to be tilted at a certain angle, if necessary, as shown in Figure 7.4.

To make sure that the signal we received as described in the preceding paragraph is that of the plasma itself but not from the background reflection of the glass tube , we must place the receiving horn out of the path of the reflected beam. This is done as shown in Figure 7.5. No reflected signal is expected with the receiving horn planted in this position.

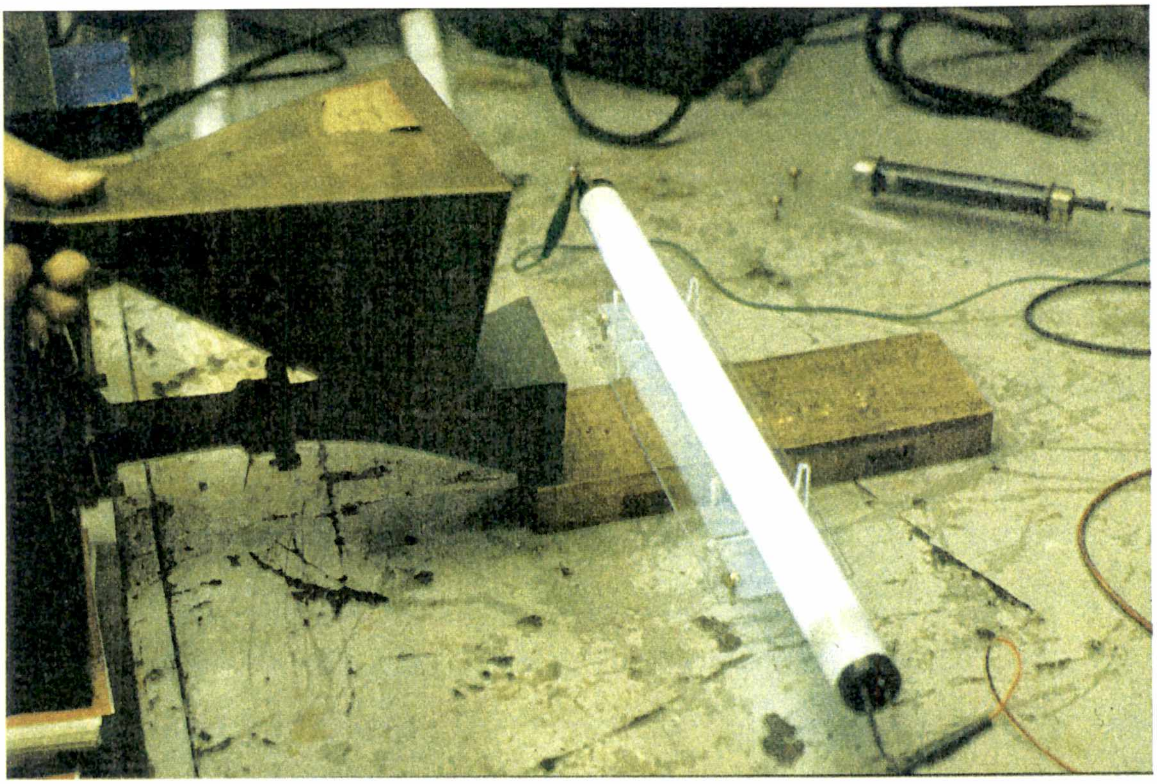

Figure 7.4 Another Position of the Receiving Horn along the Path of the Reflecting Beam.

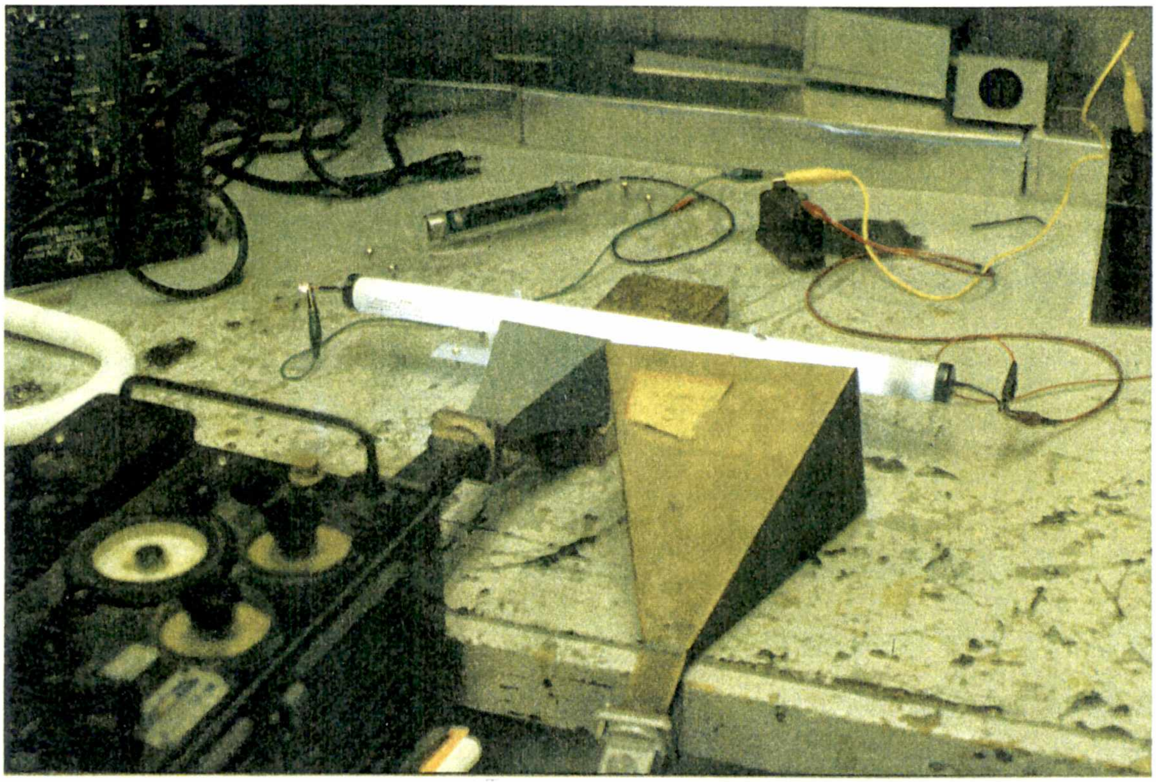

Figure 7.5 Position of the Receiving Horn out of the Path of the Reflected Beam.

Chapter 8

STEALTH PLASMA ANTENNA EXPERIMENTAL RESULTS

a) Pulsed Signal Observed along the Reflected Path

We have positioned the receiving horn along the path of the reflected beam as described in chapter 7 and Figures 7.3 and 7.4. As expected, a nice pulsed signal has been observed. The signals documented in Figures 8.1 and 8.2 correspond to the position of the horn depicted in Figures 7.3 and 7.4 respectively.

In both figures, the pulses indicate the discharging of the capacitor, and thus the plasma created inside the fluorescent tube.

When the capacitor is not discharging, and thus no plasma is created, no signal is observed. This is indicated in the horizontal flat portion of the signal.

Thus, we conclude that when plasma is on, reflection is observed. But when the plasma is off, the radar cross section is negligible.

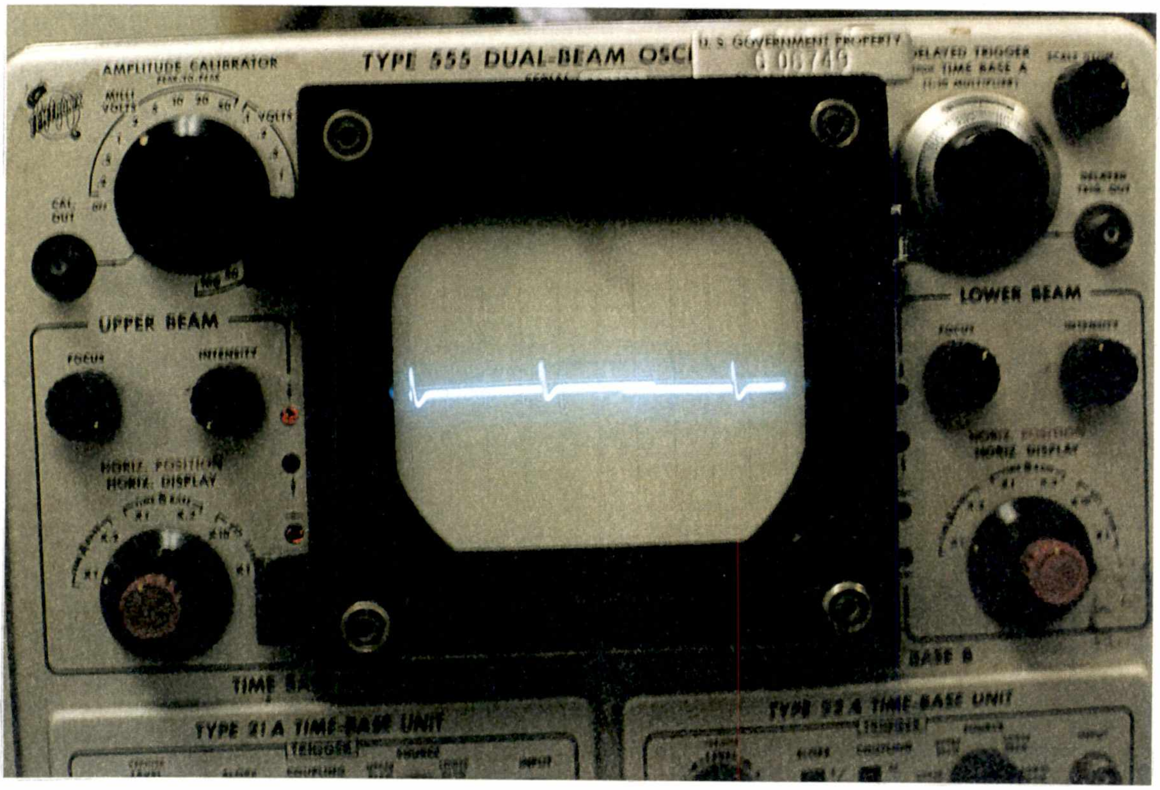

Figure 8.1 Observed Pulsed Signal Corresponding to the Receiving Horn of Figure 7.3

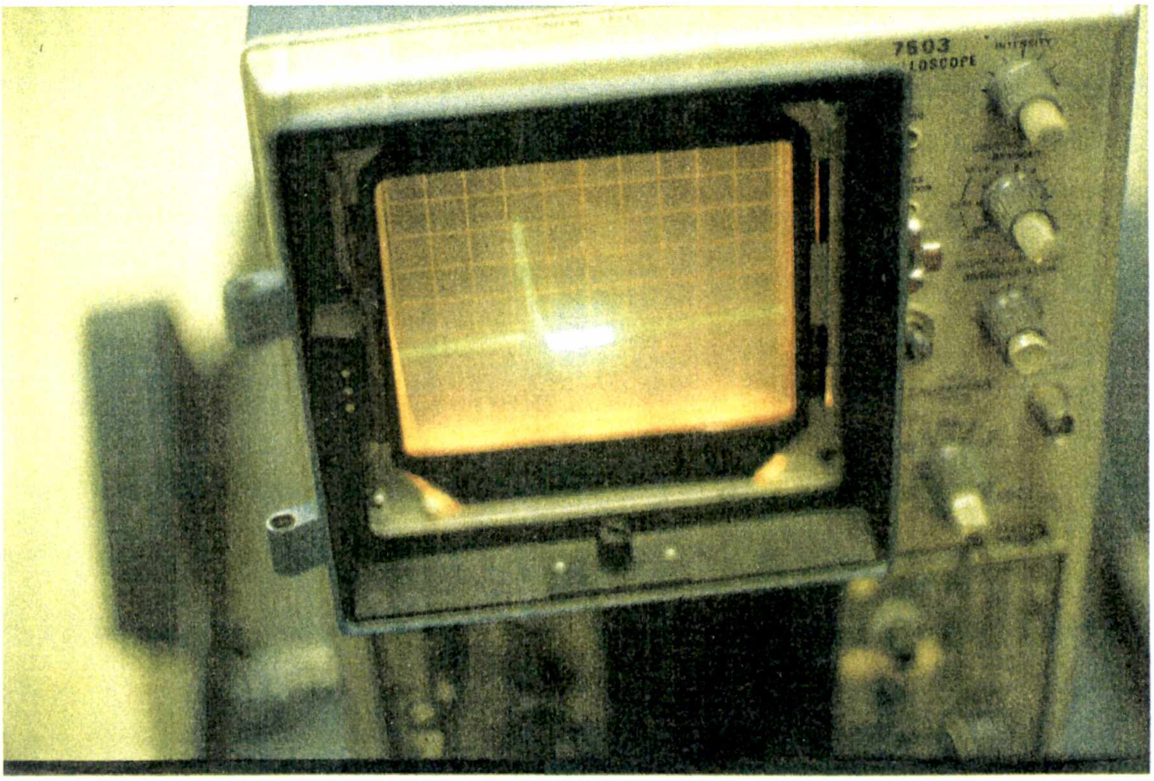

Figure 8.2 Observed Pulsed Signal Corresponding to the Receiving Horn of Figure 7.4.

b) Pulsed Signal out of the Reflected Path

We have also positioned the receiving horn out of the path of the reflected beam as depicted in Figure 7.5. As expected, no pulsed signal has been observed. This is documented in Figures 8.3 and 8.4.

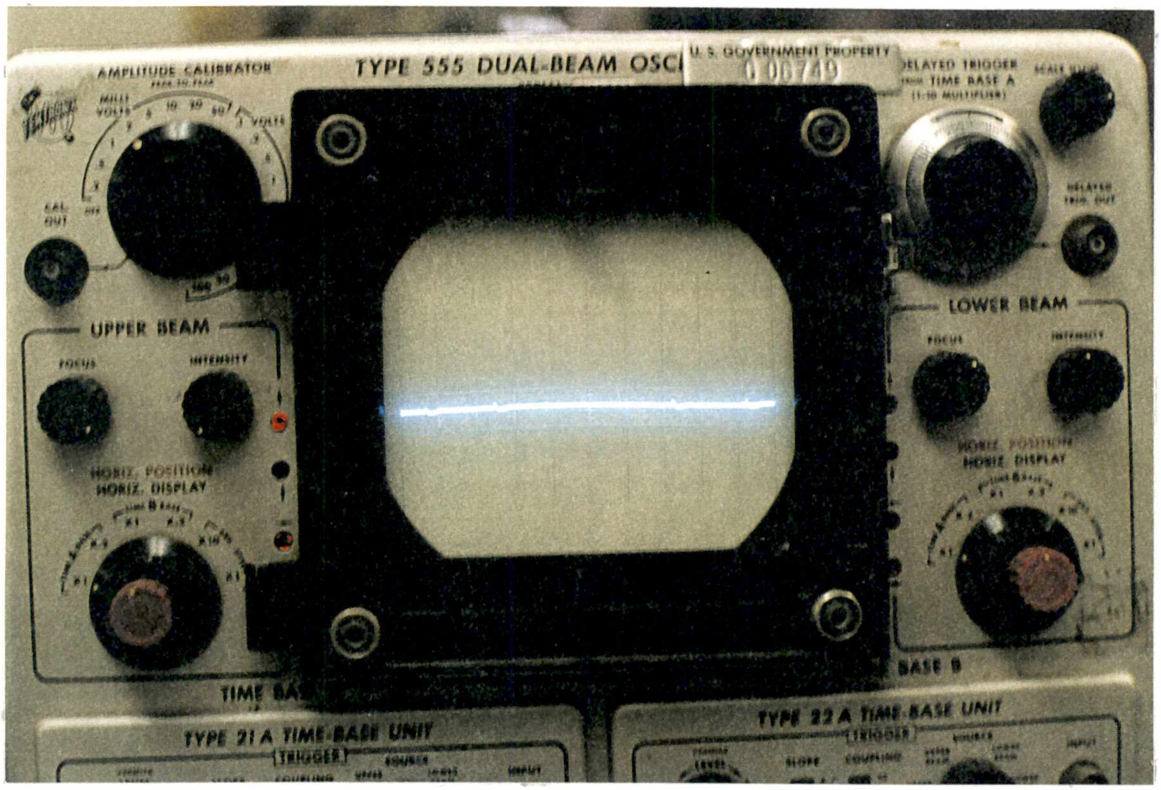

Figure 8.3 Signal Corresponding to the Receiving Horn Planted to the Left of the Transmitting Horn.

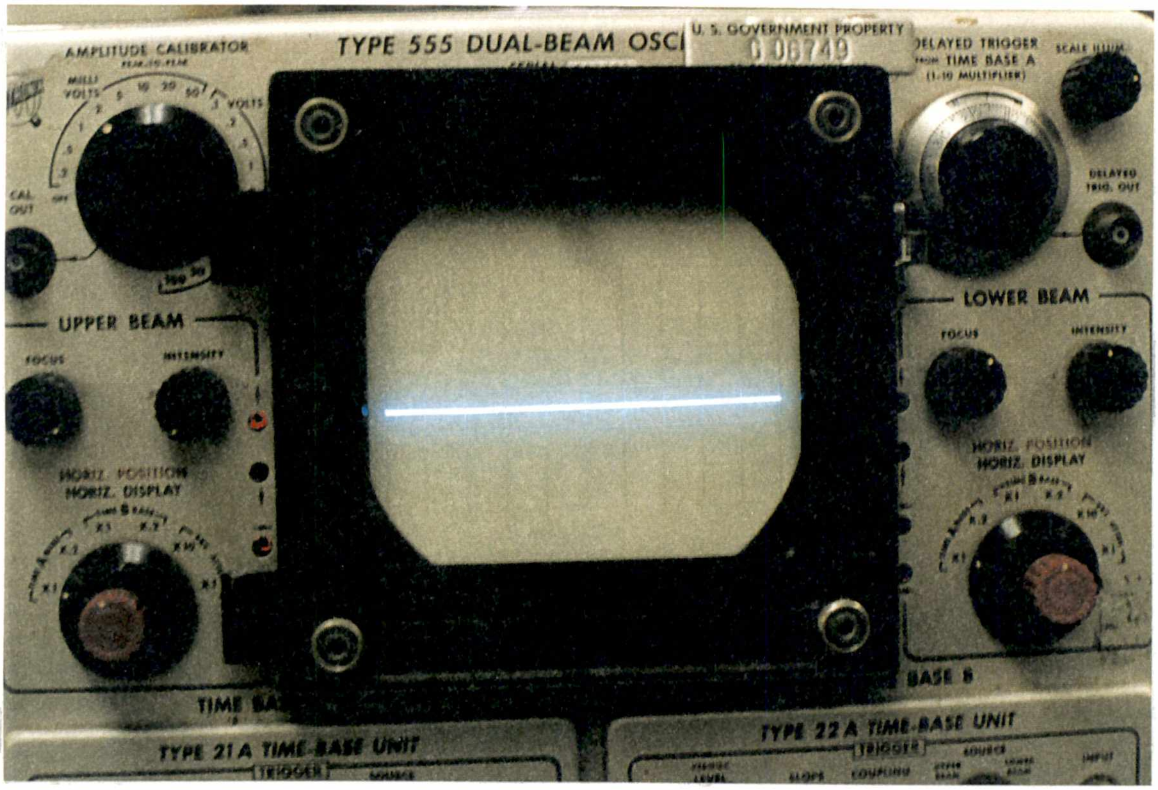

Figure 8.4 Signal Corresponding to the Receiving Horn Planted to the Right of the Transmitting Horn.

Chapter 9

CONCLUSION

a) Microwave Plasma Closing Switch

We have successfully demonstrated that it is feasible to construct an efficient coaxial plasma line structure for transmitting microwave . The relative amplitude of the signal is approximately 63 dB for the 15 MHz transmitting signal. Even for the 900 MHz transmitting signal, we have achieved a relative amplitude of 21 dB. We do not observe any significant relative amplitude gain in GHz range due to the low plasma density that can normally be created in the fluorescent tube.

Our theory based on an equivalent electrical circuit indicates that the signal will be damped. But if a correction factor representing the microwave leakage is added, our theoretical prediction fits the experimental value within acceptable experimental error of approximately 1 dB.

b) Stealth Plasma Antenna.

We have also demonstrated that it is possible to construct a stealth plasma antenna out of an ordinary fluorescent tube. When the gas is ionized inside the tube by our simple pulsed circuitry, a nice pulsed signal is observed if the receiving horn is placed along the path of the reflecting beam. No reflected signal is observed if the receiving horn is placed out of the reflecting beam path.

We conclude that when the gas is ionized , we have an efficient, highly directional receiving or transmitting antenna. When the gas de-ionizes, the structure reverts to a simple structure of glass tubes, with negligible radar cross section.

c) Limitation of Our Work

There are a few short-comings in our work.

For the microwave plasma closing switch, the theory is over-simplified. The plasma density is assumed to be uniform, while radial diffusion factor is not considered. There is also a limitation on the plasma density that can be created in a fluorescent tube. Thus, we have not tried anything beyond 900 MHz transmitting signal.

For the stealth plasma antenna, the pulsed circuitry gave us a plasma frequency of approximately 8.19 GHz . We are therefore limited by the transmitting frequency we can use.

d) Suggested Future Work

There are few things that can be done to improve our work.

1. Use a better theoretical model that takes into consideration factors such as diffusion, and the various regions that occur in the fluorescent tube.

2. Construct a structure that can give us a higher plasma density such that transmitting ability in the GHz frequency can be tested.

REFERENCES

1.1 Weng L. Kang, Mark Rader, and Igor Alexeff, " A Microwave Plasma Closing Switch and Stealth Plasma Antenna", IEEE International Conference on Plasma Science, Madison, 5-8 June, 1995, paper 2EP10.

1.2 Weng L. Kang, Mark Rader, and Igor Alexeff, " Theoretical Modeling for a Plasma Microwave Closing Switch and Plasma Stealth Antenna", to be presented in the 37th. Annual Meeting, APS Division of Plasma Physics, 6-10 Nov., 1995, Lousville, Kentucky.

2.1 Herbert P. Neff, Jr.," Introductory Electromagnetics", John Wiley & Sons, New York, 1991, p.42.

2.2 Paul Lorrain, and Dale R. Corson, "Electromagnetic Fields and Waves", 2nd. edition, W.H. Freeman and Company, San Francisco, 1972, p.297.

2.3 Herbert P. Neff, Jr., "Introductory Electromagnetics", John Wiley & Sons, New York, 1991, p.51 and p.131.

2.4 James D.Cobine, "Gaseous Conductors", Dover Publication, Inc., New York, 1958, p.124.

2.5 Earl W. McDaniel, "Collision Phenomena in Ionized Gases", John Wiley & Sons, Inc., New York, 1964, p.17.

2.6 Francis F. Chen, " Introduction to Plasma Physics and Controlled Fusion ", Volume 1: Plasma Physics, 2nd. edition, Plenum Press, New York, 1984, p.157.

2.7 David L. Book, "1990 NRL Plasma Formulary", NRL Publication 177-4405, Naval Research Laboratory, Washington DC., 1990, p.29.

3.1 " Type 491/R491 Spectrum Analyzer", Instructional Manual, Tektronix, Inc., Beaverton, Oregon, 1983, p.2-21.

4.1 Delores M. Etter, "Engineering Problem Solving with MATLAB", Prentice-Hall, Inc., Englewood Cliffs, New Jersey, 1993, p.183.

4.2 "MATLAB"' Version 4.2a., The Mathworks, Inc., Natick, Massachusetts, 1994.

5.1 Delores M. Etter, "Engineering Problem Solving with MATLAB", Prentice-Hall, Inc., Englewood Cliffs, New Jersey, 1993, p.247.

5.2 "MATLAB", Version 4.2a., The Mathworks, Inc., Natick, Massachusetts, 1994.

5.3 John Sheffield, "Plasma Scattering of Electromagnetic Radiation"' Academic Press, New York, 1975, p.29.

5.4 James D. Cobine, "Gaseous Conductors", Dover Publications, Inc., New York, 1958, p.543.

5.5 J. Reece Roth, "Industrial Plasma Engineering", Volume 1: Principles, Institute of Physics Publishing, Bristol, 1995, p.527.

5.6 Earl W. McDaniel, "Collision Phenomena in Ionized Gases", John Wiley & Sons, Inc., New York, 1964, p.35.

5.7 Francis F. Chen, "Introduction to Plasma Physics and Controlled Fusion", volume 1: Plasma Physics, 2nd. edition, Plenum Press, New York, 1984, p.7.

6.1 Mark S. Rader, "Frequency Modification of R.F. Signals Using an Ionized Gas", Ph.D. Dissertation, The University of Tennessee, Knoxville, May 1991.

6.2 David L. Book, "1990 NRL Plasma Formulary", NRL Publication 177-4405, Naval Research Laboratory, Washington DC., 1990, p.28.

6.3 J. Reece Roth, "Introduction to Fusion Energy", Ibis Publishing, Charlottesville, Virginia, 1986, p.50.

6.4 J. Reece Roth, "Introduction to Fusion Energy", Ibis Publishing, Charlottesville, Virginia, 1980, p.50.

7.1 Francis F. Chen, "Introduction to Plasma Physics and Controlled Fusion", Volume 1: Plasma Physics, 2nd. edition, Plenum Press, New York, 1984, p.350.

VITA

The author was born in Penang, Malaysia on August 2, 1947. He received the Bachelor of Science degree in Physics from The National Taiwan University in 1972. He later received the Master of Science degree in Physics from The Ohio University in 1976. After a long absence from the academic environment, he came to The University of Tennessee as a non-degree graduate student in January of 1991. He was admitted to the Master degree program in The Department of Electrical Engineering in the Fall of 1993. Since then, he has been awarded a teaching assistantship from the Electrical Engineering Department. He is now holding a research assistantship from Professor Igor Alexeff and is planing to continue for the Ph.D. study.